BER Reduction of OFDM Based Broadband Communication Systems over Multipath Channels with Impulsive Noise

M. Mirahmadi, *Member, IEEE*, A. Al-Dweik, *Senior Member, IEEE*, and A. Shami, *Senior Member, IEEE*

***Abstract*—This paper presents an efficient technique to jointly mitigate the severe bit error rate (BER) performance degradation caused by impulsive noise (IN) and multipath fading in broadband transmission systems. The proposed system is based on a low complexity interleaving process applied after the inverse fast Fourier transform (IFFT) in orthogonal frequency division multiplexing (OFDM) systems, hence it is denoted as time-domain interleaving (TDI). The proposed TDI introduces both time and frequency diversity, which can be used to effectively combat impairments such as IN and frequency-selective fading. In addition to its substantial BER reduction capability, the TDI does not degrade the spectral efficiency and has low computational complexity. In frequency-selective fading channels, the BER of the proposed system is mathematically equal to that of Walsh-Hadamard precoded OFDM systems [1]. In presence of IN, analytical and simulation results show that TDI can remarkably reduce the level of the error floors that are commonly observed. Specifically, TDI can achieve a BER of 10^{-5} for less than 1 dB difference from the IN-free case.**

***Index Terms*—OFDM, interleaving, diversity, precoding, fading, impulsive noise, Walsh-Hadamard.**

I. Introduction

ORTHOGONAL frequency division multiplexing (OFDM) is a multicarrier modulation technique that employs orthogonal subcarriers. Due to the unique features of OFDM, it is currently adopted in several wireless communication standards such as digital audio broadcasting (DAB) [2], digital video broadcasting-terrestrial (DVB-T) [3], worldwide interoperability for microwave access (WiMAX) technologies [4] and the 4G LTE-Advanced [5].

Besides its superiority for wireless transmission, OFDM has rendered itself as the dominant modulation technique for many wired technologies and standards such as the second generation digital video transmission over cable (DVB-C2) [6], the asymmetric digital subscriber line (ADSL) [7] and home networking over power line communications (PLC) [8]. For such applications, the main advantage of using OFDM is the bandwidth efficiency and reduced system complexity as a result of using the fast Fourier transform (FFT) and its inverse version (IFFT).

However, for both wired and wireless transmission, the frequency-selective fading remained one of the major factors that can cause severe bit error performance degradation to OFDM systems. Therefore, tremendous efforts have been devoted in the literature to alleviate the effect of fading using various techniques. Among many others, precoded OFDM [9] and modulation diversity techniques [10]- [11] have demonstrated significant robustness in severe frequency-selective channel.

In addition to the multipath propagation phenomenon, which is a major source of disturbance for several communication systems, impulsive noise (IN) is another significant source of disturbance for particular OFDM based applications such as DVB-T [12]–[14], PLC [15] and ADSL systems [16]. Unlike multipath fading, adopting OFDM for IN channels might impact the performance negatively [17], because an impulsive burst may destroy all subcarriers within the OFDM symbol due to the averaging process of the FFT. Hence, using OFDM for IN channels must be accompanied with effective IN mitigation techniques [18]. In the literature, the common IN mitigation techniques used for single carrier systems such as clipping and blanking are extended to OFDM systems [15]. Approaches that are designed specifically for OFDM systems are reported in the literature as well. For example, Abedlkefi *et al*. [19] exploited the pilots embedded within OFDM signals to detect and correct the samples contaminated by IN. Zhidkov [17] proposed a frequency domain IN cancellation technique for DVB-T systems where the IN is estimated and subtracted after the FFT.

In general, most of the aforementioned techniques suffer from limited performance improvement, particularly in heavily distributed IN channels. Moreover, most of the systems reported in the literature assume that the IN bursts have a short duration that is equal to the OFDM sample period, and hence, all IN samples can be considered uncorrelated [15]–[20]. Although such assumption is pivotal to enable analytical performance evaluation, it does not capture the bursty nature of the IN, which is confirmed by channel measurements for various applications [16], [21], [22], particularly for broadband communications where the OFDM sample duration is very short [8]. For example, the OFDM symbol duration as defined by the IEEE 1901 PLC standard [8] is only 5.12 μs. Hence, even very narrow bursts can affect several consecutive OFDM

Manuscript received March 26, 2013; revised August 21 and September 28, 2013. The editor coordinating the review of this paper and approving it for publication was A. Tonello.

M. Mirahmadi and A. Shami are with the Department of Electrical and Computer Engineering, Western University, London, Ontario, Canada (e-mail: {mmirahma, ashami2}@uwo.ca).

A. Al-Dweik is with the Department of Electrical and Computer Engineering, Khalifa University, Abu Dhabi, UAE (e-mail: dweik@kustar.ac.ae). He is also with the School of Engineering, University of Guelph, Guelph, Ontario, Canada (e-mail: aaldweik@uoguelph.ca).

This work was conducted when A. Al-Dweik was a Visiting Professor at Western University, London, ON, Canada.

Digital Object Identifier 10.1109/TCOMM.2013.102313.130220

samples [21], or even the entire OFDM symbol. Consequently, most of the techniques that are designed based on the assumption of uncorrelated samples might not be effective in the presence of IN bursts.

In [23], Al-Dweik *et al.* proposed a new OFDM symbol structure to combat IN by interleaving the time-domain samples after the IFFT process. The technique, namely Time-Domain Interleaving (TDI), was then extended in [24] to include multipath fading channels. However, the results in [23] and [24] were entirely obtained via Monte Carlo simulation using the assumption of ideal IN samples detection and blanking. It is worth noting that both TDI and the system reported in [11] interleave a block of OFDM symbols before transmission, however the two systems are fundamentally different. The system described in [11] jointly modulates all symbols in the block and then interleaves the modulated symbols, whereas the TDI modulates the information bits conventionally, applies the IFFT and then interleaves the block.

This paper presents a novel technique, based on TDI [23], in conjunction with a two-level threshold-based blanking scheme to combat the adverse effects of multipath propagation as well as IN for OFDM based communications systems. Unlike traditional interleaved single carrier and OFDM systems where the information symbols are spread over a larger number of transmission blocks [25], the TDI system interleaves the time domain samples after the IFFT which are composed of a mixture of all information symbols. This results in a significant improvement in uncoded BER that can never be achieved with conventional interleaving. To the best of our knowledge, the proposed TDI has never been considered in the literature. In addition, unlike the traditional IN mitigation techniques, the use of the proposed blanking scheme in conjunction with TDI enables the proposed system to efficiently combat IN even in frequency-selective channels. Closed-form formulae are derived for the signal-to-interference and noise ratio (SINR) in frequency-selective fading channels using zero forcing (ZF) and minimum mean squared error (MMSE) equalizers. Analytical and simulation results reveal that the proposed TDI system offers a remarkable BER performance improvement and can effectively and jointly combat the IN bursts and multipath fading. It is worth noting that in frequency-selective fading channels without IN, TDI can achieve the same BER as Walsh-Hadamard precoded OFDM systems [1], [9]. In addition, it significantly outperforms such systems in the presence of IN.

The rest of this paper is organized as follows. The system and channel models are presented in Section II. The proposed system model is described in Section III. Section IV presents the symbol blanking scheme suggested to mitigate the IN effects. The system performance analysis in fading channels using ZF and MMSE equalizers are provided in Sections V and VI, respectively. The numerical results are given in Section VII, and finally Section VIII concludes the paper.

Notations **:** In what follows unless otherwise specified, uppercase boldface and blackboard letters, such as $\mathbf{H}$ and $\mathbb{H}$, will denote $N \times N$ matrices, whereas lowercase boldface letters, such as $\mathbf{x}$, will denote row or column vectors with N elements. Samples or data symbols from the ℓth OFDM symbol will be denoted using lower case letters such as y. Symbols with a hat such as $\hat{x}$ will denote the estimate of x, and symbols with breve $\breve{\mathbf{x}}$ denotes an interleaved sequence. Moreover, $x \sim \mathcal{N}$, $\mathcal{N}_c$, $\mathcal{U}$ and $\mathcal{B}$ will denote that random variable x follows the normal, complex normal, uniform or Bernoulli distribution, respectively. The expectation, Hermitian transpose and conjugation are denoted as $E[\cdot]$, $[\cdot]^H$ and $[\cdot]^*$.

II. OFDM System and Channel Models

A. OFDM System Model

Consider an OFDM system with N subcarriers modulated by a sequence of N complex data symbols $\mathbf{d} = [d_0, d_1, ..., d_{N-1}]^T$. The data symbols are selected uniformly from a particular constellation such as quadrature amplitude modulation (QAM). The modulation process can be implemented efficiently using N-points IFFT, where the IFFT output during the ℓth OFDM block $\mathbf{x}(\ell) = \mathbf{F}^H \mathbf{d}(\ell)$. Matrix $\mathbf{F}$ is the normalized FFT matrix whose elements are defined as $F_{i,k} = \kappa e^{-\omega i k}$, $\kappa = 1/\sqrt{N}$, $\omega = \mathrm{j}2\pi/N$, $\mathrm{j} = \sqrt{-1}$ and $\{i, k\} = 0, 1, ..., N-1$ denote the row and column numbers, respectively. Since $\mathbf{F}$ is a unitary matrix, then $\mathbf{F}^H = \mathbf{F}^{-1}$. Consequently, the nth sample in $\mathbf{x}$ can be expressed as

$$x_n(\ell) = \kappa \sum_{i=0}^{N-1} d_i(\ell) e^{\omega i n}, \quad n = 0, 1, ..., N-1. \quad (1)$$

To eliminate the inter-symbol-interference (ISI) between consecutive OFDM symbols in frequency-selective multipath fading channels, a cyclic prefix (CP) of length $\bar{N}$ samples no less than the normalized channel delay spread (L_h) is formed by copying the last $\bar{N}$ samples of $\mathbf{x}$ and appending them at the front of $\mathbf{x}$ to compose the transmission symbol with a total length $N_t = N + \bar{N}$ samples and a duration of T_t seconds. Hence, the complex baseband symbol transmitted during the ℓth signaling period can be expressed as

$$\tilde{\mathbf{x}}(\ell) = [x_{N-\bar{N}}(\ell), x_{N-\bar{N}+1}(\ell),..., x_{N-1}(\ell), x_0(\ell), x_1(\ell), \ldots, x_{N-1}(\ell)]^T. \quad (2)$$

Consequently, the ith transmitted sample $\tilde{x}_i(\ell) = x_{\langle i-\bar{N}\rangle}(\ell)$, $i = 0, 1, ..., N_t-1$, where $\langle i\rangle \triangleq i \bmod N$. Then, the sequence $\tilde{\mathbf{x}}$ is upsampled, filtered and up-converted to a radio frequency centered at f_c.

At the receiver frontend, the received signal is down-converted to baseband and sampled at a rate $T_s = T_t/N_t$. In this work, we assume that the channel is composed of $L_h + 1$ independent multipath components each of which has a gain h_m and delay $m \times T_s$, where $m \in \{0, 1,..., \bar{N}\}$. The channel taps are assumed to be constant over N OFDM symbols, which corresponds to quasi-static multipath fading channels. The received sequence $\tilde{\mathbf{y}} = \tilde{\mathbb{H}}(\ell)\tilde{\mathbf{x}}(\ell) + \tilde{\mathbf{z}}(\ell)$, where the channel matrix $\tilde{\mathbb{H}}$ is an $N_t \times N_t$ Toeplitz matrix with h_0 on the principal diagonal and h_1,..., h_{L_h} on the minor diagonals, respectively [27] and $\tilde{\mathbf{z}}(\ell)$ represents the overall additive noise that includes AWGN and IN. For notations' simplicity, we omit the subscript ℓ in the remaining parts of this section. Given that $L_h < \bar{N}$, the nth sample of $\tilde{\mathbf{y}}$ can be expressed as $\tilde{y}_n = \sum_{i=0}^{L_h} h_i\, x_{\langle n-i-\bar{N}\rangle} + z_n$. Subsequently, the receiver should identify and extract the sequence $\mathbf{y} = [\tilde{y}_{\bar{N}}, \tilde{y}_{\bar{N}+1}, \ldots, \tilde{y}_{N+\bar{N}-1}]$ and discard the first $\bar{N}$ CP samples $[\tilde{y}_0, \tilde{y}_1, \ldots, \tilde{y}_{\bar{N}-1}]$. Therefore,

$$y_n = \sum_{i=0}^{L_h} h_i\, x_{\langle n-i\rangle} + z_{n+\bar{N}}, \quad 0 \le n \le N-1. \quad (3)$$

In vector notation, the sequence $\mathbf{y}$ can be expressed as

$$\mathbf{y} = \mathbb{H}\mathbf{x} + \mathbf{z} \tag{4}$$

where $\mathbf{z} = [z_{\bar{N}}, z_{\bar{N}+1}, \cdots, z_{\bar{N}+N-1}]^T$, and the channel matrix $\mathbb{H}$ is circulant [27], [28]. It is worth noting that the quasi-static channel model, and hence the proposed system can be adopted for several broadband OFDM systems where the channel changes at a rate lower than the interleaved block length. Examples for such system include the DVB-T [12]- [14], PLC [15] and ADSL systems [16]. For OFDM systems where the channel might change faster than the interleaver depth, higher complexity solutions such as time-domain equalization, or interleaver depth optimization might be invoked.

B. Impulsive Noise Model

The IN is usually characterized by bursts of one or more short pulses whose amplitude g, duration T_I, and time of occurrence are all random parameters. The main models used for the amplitude distribution are the Middleton class-A [29], exponential [21] and Gaussian [30]. The common distributions of the bursts' arrival process are partitioned Markov chains (PMC) [21], Gated Bernoulli-Gaussian (GBG) [30], and Poisson [22]. The burst width distribution is usually modeled using the PMC or as the sum of two lognormal random variables [16].

To enable analytical performance evaluation over IN channels, the GBG model is widely adopted in the literature where the IN is modeled as a sequence of independent, Bernoulli distributed bursts with equal and fixed width, which is equal to the duration of a single time-domain OFDM sample [18], [19], [30]. Hence, the overall noise samples at the receiver frontend $z_n = w_n + \rho_n g_n$, where the AWGN $w_n \sim \mathcal{N}_c\left(0, \sigma_w^2\right)$ and $\sigma_w^2 = E\left[|w_n|^2\right] = N_0/2$. The IN component $\rho_n g_n$ is modeled as a gated Gaussian process, and $\rho_n \sim \mathcal{B}\{0,1\}$ where $p = P\{\rho_n = 1\}$, and $g_n \sim \mathcal{N}_c\left(0, \sigma_g^2\right)$ where $\sigma_g^2 \gg \sigma_w^2$ [18].

In this work, the GBG model is adopted to represent the IN, which is modeled as a sequence of independent bursts each of which consists of $1 \leq \varkappa \leq N + \bar{N}$ pulses. In general, the burst width $\varkappa$ is a random variable whose distribution can be modeled as a uniform or lognormal distribution, or by using PMC [16]. Therefore, the overall received noise $\mathbf{z} = \mathbf{w} + \rho \mathbf{b}\,\mathbf{g}$, where $\mathbf{z} = [z_0, z_1, ..., z_{N+\bar{N}-1}]$. The vector $\mathbf{b}$ is used to specify the position as well as the width of the IN burst with respect to the OFDM symbol. Given that n_0 is the index of the first OFDM sample that is affected by a noise burst, then the elements of $\mathbf{b}$ are

$$b_n = \begin{cases} 1, & n_0 \leq n < n_0 + \varkappa \\ 0, & \text{otherwise} \end{cases}, \tag{5}$$

where $n_0 \sim \mathcal{U}\left[0, N + \bar{N} - \varkappa\right]$. Therefore, the location of the noise burst will be random and uniformly distributed over the OFDM symbol period. Thus, any IN burst can affect a maximum of one OFDM symbol.

III. Proposed System Model

The proposed system is similar to the conventional OFDM system described in Section II. However as depicted in Fig. 1, after the IFFT, N OFDM symbols are interleaved using a simple row/column interleaver,

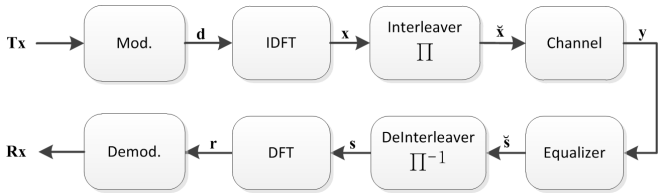

Fig. 1. The proposed TDI system in fading channels.

$$\overbrace{\qquad\qquad\qquad\qquad}^{read}$$
$$write\begin{cases} x_0(0) & x_0(1) & \cdots & x_0(N-1) \\ x_1(0) & x_1(1) & \cdots & x_1(N-1) \\ \vdots & \vdots & & \\ x_{N-1}(0) & x_{N-1}(1) & \cdots & x_{N-1}(N-1) \end{cases}. \tag{6}$$

It is worth noting that using the block interleaver represented in (6) simplifies the analysis, but the delay of a pair of such interleaver/deinterleaver is equal to $2N$ OFDM symbols. Alternatively, convolutional interleaving can offer the same BER performance with only half of that delay [32, p. 467].

The interleaver produces N interleaved symbols $\{\check{\mathbf{x}}(0), \check{\mathbf{x}}(1), ..., \check{\mathbf{x}}(N-1)\}$ where

$$\check{\mathbf{x}}(\ell) = \left[\begin{array}{cccc} \check{x}_\ell(0) & \check{x}_\ell(1) & \cdots & \check{x}_\ell(N-1) \end{array}\right]^T. \tag{7}$$

The CP samples are formed by copying the last $\bar{N}$ samples of $\check{\mathbf{x}}$ and appending them at the front of $\check{\mathbf{x}}$ to compose the transmission symbol. Hence, the complex baseband symbol transmitted during the ℓth signaling period can be expressed as

$$\tilde{\mathbf{x}}(\ell) = [\check{x}_\ell(N-\bar{N}), \check{x}_\ell(N-\bar{N}+1), ..., \check{x}_\ell(N-1), \check{x}_\ell(0)\ , \check{x}_\ell(1), \ldots, \check{x}_\ell(N-1)]^T. \tag{8}$$

Consequently, the ith transmitted sample is $\tilde{x}_i(\ell) = \check{x}_\ell(\langle i - \bar{N}\rangle)$, $i = 0, 1, ..., N_t - 1$. The remaining transmission and reception processes are similar to conventional OFDM systems. Therefore, the received sequence $\tilde{\mathbf{y}}(\ell) = \tilde{\mathbb{H}}(\ell)\tilde{\mathbf{x}}(\ell) + \tilde{\mathbf{z}}(\ell)$, where $\tilde{y}_n = \sum_{i=0}^{L_h} h_i\, \check{x}_\ell(\langle n - i - \bar{N}\rangle) + z_n$. Subsequently, after discarding the first $\bar{N}$ CP samples, the remaining samples can be expressed as

$$\check{y}_n = \sum_{i=0}^{L_h} h_i\, \check{x}_\ell(\langle n - i\rangle) + z_{n+\bar{N}}, \qquad 0 \leq n \leq N-1. \tag{9}$$

In vector notation $\check{\mathbf{y}} = \mathbb{H}\check{\mathbf{x}} + \mathbf{z}$. To simplify the discussion, assume initially that the channel matrix $\mathbb{H}$ is the identity matrix. Therefore, the received N samples, after removing the CP, can be written as

$$\check{\mathbf{y}}(\ell) = \check{\mathbf{x}}(\ell) + \mathbf{w}(\ell) + \rho(\ell)\mathbf{b}(\ell)\mathbf{g}(\ell). \tag{10}$$

By noting that the deinterleaving process interleaves the vectors $\mathbf{w}(\ell)$, $\mathbf{b}(\ell)$ and $\mathbf{g}(\ell)$, the deinterleaving process yields

$$\mathbf{y}(\ell) = \mathbf{x}(\ell) + \check{\mathbf{w}}(\ell) + \check{\rho}(\ell)\check{\mathbf{b}}\,(\ell)\check{\mathbf{g}}(\ell) \tag{11}$$

where $\check{\mathbf{w}}$ and $\check{\mathbf{g}}$ are the interleaved AWGN and IN vectors. The burst and sample gating factors $\check{\rho}$ and $\check{\mathbf{b}}$ have different properties from the original ρ and $\mathbf{b}$. For example, given that $\rho(0) = 1$ and $\varkappa = N_t$, then $\check{\rho}(\ell) = b_0(\ell) = 1$ $\forall \ell \in \{1, 2, ...N\}$, *i.e.*, the first sample of every OFDM symbol

after deinterleaving will be affected by an IN pulse, while all other samples in all symbols will be IN free. Consequently, the FFT output can be expressed as

$$r_k(\ell) = \kappa \sum_{n=0}^{N-1} y_n(\ell) e^{-\omega nk},\ k = 0,\ 1,\ ...,\ N-1 \quad (12)$$

which can be reduced to

$$r_k(\ell) = d_k(\ell) + \psi_k(\ell) + u_k(\ell) \quad (13)$$

where the FFT of the AWGN $\psi_k \sim \mathcal{N}_c\left(0, \sigma_w^2\right)$. The last term in (13) represents the FFT of the IN

$$u_k(\ell) = \kappa \breve{\rho}(\ell) \sum_{n=0}^{N-1} \breve{b}_n(\ell) \breve{g}_n(\ell) e^{-\omega nk}$$

where $u_k \sim \mathcal{N}_c\left(0, \sigma_u^2\right)$, and

$$\begin{aligned} \sigma_u^2 &= \kappa^2 \breve{\rho}(\ell) \sigma_g^2 \sum_{n=0}^{N-1} \breve{b}_n(\ell) \\ &= \kappa^2 \breve{\rho}(\ell) \sigma_g^2 \breve{\varkappa}(\ell) \end{aligned} \quad (14)$$

where $\breve{\varkappa} \neq \varkappa$ is the number of nonzero elements in the vector $\breve{\mathbf{b}}(\ell)$, *i.e.*, the Hamming weight of $\breve{\mathbf{b}}(\ell)$.

It can be concluded from (13) and (14) that the deinterleaving process spreads the IN burst over most OFDM symbols within the deinterleaved block. The FFT process applied after the deinterleaving averages the IN pulses over all subcarriers within a given OFDM symbol, which may cause the loss of up to $\varkappa$ OFDM symbols because $\sigma_g^2 \gg \sigma_w^2$ [18], [21], [38]. It is also worth noting that the interleaving process described in (6) does not affect the peak-to-average power ratio (PAPR) of the transmitted signal because the interleaver changes the order of the transmitted samples without changing their values.

IV. TDI Symbol Blanking

An efficient solution to mitigate the effects of impulse noise is to apply blanking [15], [17], where the received samples with high amplitudes are set to zero. The contaminated samples are detected and suppressed by comparing the received samples' values with a particular threshold $\mathcal{T}_1$. Therefore, the output of the blanking nonlinearity is $\breve{q}_n = \breve{y}_n\ \forall\ |\breve{y}_n| \leq \mathcal{T}_1$ and 0 otherwise. We refer to this approach as sample-by-sample blanking. After blanking and deinterleaving, the nth sample of the FFT input $q_n = y_n\ \forall\ |y_n| \leq \mathcal{T}_1$ and 0 otherwise, where $y_n = x_n + w_n + \rho b_n\, g_n$. Therefore, the FFT output $\mathbf{s}(\ell) = \mathbf{F}\mathbf{q}(\ell)$ and the kth subcarrier can be written as

$$\begin{aligned} s_k(\ell) &= \kappa \sum_{n=0}^{N-1} q_n(\ell) e^{-\omega nk},\ k = 0,\ 1,\ ...,\ N-1 \\ &= \kappa \sum_{n \in \mathcal{C}} y_n(\ell) e^{-\omega nk} \end{aligned} \quad (15)$$

where $\mathcal{C} = \{n \in \{0, 1, ..., N-1\} | q_n \neq 0\}$. The average error probability can be expressed as

$$P_e = \sum\nolimits_{\mathcal{C}} P(e|\mathcal{C}) P(\mathcal{C}). \quad (16)$$

The sample blanking threshold $\mathcal{T}_1$ should be selected to minimize the BER, and it is a function of several variables such as signal-to-noise ratio (SNR), signal-to-IN ratio (SIR) and $\varkappa$ [15]. It is worth noting that the blanking process is not ideal in the sense that it will not necessarily blank all IN samples, and may blank some information samples, which is due to the high peak-to-average-power-ratio (PAPR) problem inherent in OFDM systems [31]. In addition, the sample-by-sample blanking is not feasible in frequency-selective channels due to the vast amplitude fluctuations that a signal may experience in such channels [19].

In our study we observed that despite the fact that detecting corrupted samples is very challenging, the corrupted symbols can be easily and accurately identified by introducing an additional threshold $\mathcal{T}_2$ for the blanking process, where $\mathcal{T}_2$ denotes the number of samples with amplitudes larger than $\mathcal{T}_1$. In each symbol, if the number of samples with $|y_n| \geq \mathcal{T}_1$ exceeds $\mathcal{T}_2$, the entire symbol is considered corrupted and is blanked subsequently. *i.e.*,

$$\tilde{\mathbf{q}} = \begin{cases} 0 \times \tilde{\mathbf{y}} & \sum_n \mathbf{1}_{\{|\tilde{y_n}| > \mathcal{T}_1\}} > \mathcal{T}_2 \\ \tilde{\mathbf{y}} & \text{otherwise} \end{cases} \quad (17)$$

This approach is called symbol blanking for the rest of the paper. It is worth mentioning that the time diversity provided by the TDI interleaving mechanism enables us to recover the blanked symbol and allows symbol blanking without any significant loss.

It is worth noting the symbol blanking substantially relaxes the system sensitivity to $\mathcal{T}_1$, which is difficult to estimate accurately in conventional OFDM systems [20], [39].

Based on the widely used assumption that $\sigma_g^2 \gg \sigma_w^2$ [18], [21], [38], the symbol blanking process is expected to be highly accurate. By assuming a perfect burst detection process, the average probability of error over a block of N symbols can be expressed as

$$P_e = \sum\nolimits_{\epsilon=0}^{N-1} P(e|\epsilon) P(\epsilon) \quad (18)$$

where ϵ denotes the total number of IN bursts per block of N OFDM symbols, which has a binomial PDF

$$P(\epsilon = i) = \binom{N}{i} p^i (1-p)^{N-i} \quad (19)$$

where p is the probability of the occurrence of IN during each symbol period. The exact value of p can be measured or extracted from the selected IN model.

It is worth mentioning that the analyses in the next sections are valid for any IN model that considers IN bursts longer than the sample period. Since symbol blanking technique blocks the corrupted symbols, the exact amplitude of the IN is not a contributing factor in the performance, as long as the symbols that are hit by IN can be correctly detected. To ensure that this condition remains true, the thresholds $\mathcal{T}_1$ and $\mathcal{T}_2$ have to be carefully adjusted.

V. System Performance using ZF Equalizer

As it can be noted from (18), the probability of error is computed as the average of all possible symbol blanking scenarios. A particular case of interest is the one where $\epsilon = 0$, which corresponds to an IN-free frequency-selective fading channel. Therefore, we first consider the case of $\epsilon = 0$, then the results are generalized for $\epsilon > 0$. The TDI system block diagram is given in Fig. 1 for notation clarification.

A. No Samples Blanked, $\epsilon = 0$

The receiver design can be performed by noting that $\mathbb{H} = \mathbf{F}^H \mathbf{H} \mathbf{F}$ [40], where

$$\mathbf{H} = \mathrm{diag}\left([H_0,\ H_1,\ \cdots,\ H_{N-1}]\right),\ H_k = \sum_{m=0}^{L_h} h_m e^{-\omega mk}.$$

Thus (4) can be written as

$$\breve{\mathbf{y}} = \mathbf{F}^H \mathbf{H} \mathbf{F} \breve{\mathbf{x}} + \mathbf{w}. \quad (20)$$

Therefore, the ZF equalizer output can be written as $\breve{\mathbf{s}} = \mathbf{F}^H\mathbf{H}^{-1}\mathbf{F}\breve{\mathbf{y}} = \breve{\mathbf{x}}+\mathbb{V}\mathbf{w}$, where $\mathbb{V} \triangleq \mathbf{F}^H\mathbf{H}^{-1}\mathbf{F}$. However, since $\mathbf{H}^{-1}$ is a diagonal matrix,

$$\mathbf{H}^{-1} = \mathrm{diag}\left(\left[\frac{1}{H_0}, \frac{1}{H_1}, \cdots, \frac{1}{H_{N-1}}\right]\right) \tag{21}$$

and matrix $\mathbb{V}$ is circulant, the first row of $\mathbb{V}$, using the Matlab notations, is given by

$$\mathbb{V}(0,:)=\kappa^2\begin{bmatrix} \sum_{k=0}^{N-1}\frac{1}{H_k} \\ \sum_{k=0}^{N-1}\frac{\mathrm{e}^{-\omega k}}{H_k} \\ \vdots \\ \sum_{k=0}^{N-1}\frac{\mathrm{e}^{-(N-1)\omega k}}{H_k} \end{bmatrix}^T. \tag{22}$$

It can be noted from (22) that each element in $\mathbb{V}$ is composed of a mixture of all elements of $\mathbf{H}^{-1}$. Specifically, each row in $\mathbb{V}$ consists of the FFT of the vector $\left[\frac{1}{H_0}, \frac{1}{H_1}, \cdots, \frac{1}{H_{N-1}}\right]$. Consequently, the term $\mathbb{V}\mathbf{w} \triangleq \breve{\mathbf{\Phi}}$ is given by

$$\breve{\mathbf{\Phi}} =\kappa\begin{bmatrix} \sum_{i=0}^{N-1} w_i\Delta_i \\ \sum_{i=0}^{N-1} w_i\Delta_{\langle i-1\rangle} \\ \vdots \\ \sum_{i=0}^{N-1} w_i\Delta_{\langle i+1\rangle} \end{bmatrix} \tag{23}$$

where $\Delta_i = \sum_{k=0}^{N-1}\frac{e^{-\omega ki}}{H_k}$. After deinterleaving, the ℓth OFDM symbol $\mathbf{s}(\ell)= \mathbf{x}(\ell) + \mathbf{\Phi}(\ell)$, where $\mathbf{x}(\ell) = \mathbf{F}^H\mathbf{d}(\ell)$ and $\mathbf{\Phi}$ is formed by equalizing and deinterleaving the additive noise,

$$\mathbf{\Phi}(\ell) = \kappa\begin{bmatrix} \sum_{i=0}^{N-1} w_i(0)\Delta_{\langle -\ell+i\rangle}(0) \\ \sum_{i=0}^{N-1} w_i(1)\Delta_{\langle -\ell+i\rangle}(1) \\ \vdots \\ \sum_{i=0}^{N-1} w_i(N-1)\Delta_{\langle -\ell+i\rangle}(N-1) \end{bmatrix}. \tag{24}$$

The FFT is then applied to extract the decision variables $\mathbf{r}(\ell) = \mathbf{d}(\ell) + \mathbf{F}\mathbf{\Phi}(\ell)$.

As an example, for the case of $\ell = 0$, the noise component can be described as

$$\mathbf{F}\mathbf{\Phi}(0) = \kappa^2\begin{bmatrix} \sum_{j,i=0}^{N-1} w_i(j)\Delta_i(j) \\ \sum_{j,i=0}^{N-1} w_i(j)\Delta_i(j)\mathrm{e}^{-\omega j} \\ \vdots \\ \sum_{j,i=0}^{N-1} w_i(j)\Delta_i(j)\mathrm{e}^{-(N-1)\omega j} \end{bmatrix}. \tag{25}$$

Since all samples are identically distributed, without loss of generality, we consider the first subcarrier of the first OFDM symbol, which is given by

$$r_0(0) = d_0(0) + \kappa^2\sum_{j=0}^{N-1}\sum_{i=0}^{N-1} w_i(j)\Delta_i(j). \tag{26}$$

Substituting the value of Δ_i and noting that $H_k(\ell) = H_k$ $\forall\ell$ for the considered quasi-static channel, then (26) can be written as

$$r_0(0) = d_0(0) + \kappa^2\sum_{j=0}^{N-1}\sum_{i=0}^{N-1}\sum_{k=0}^{N-1}\frac{e^{-\omega ki}}{H_k}w_i(j). \tag{27}$$

By comparing (27) to the standard OFDM, which has

$$r_0^{std} = d_0 + \frac{\kappa^2}{H_0}\sum_{i=0}^{N-1} w_i. \tag{28}$$

It can be noted that the channel frequency response at each subcarrier in the TDI system is a mixture of the channel frequency responses H_i of the entire interleaving block length, which is caused by the deinterleaving and the last FFT operations.

The conditional SNR for a given channel matrix $\mathbf{H}$ can be expressed as

$$\mathrm{SNR}\,|_{\mathbf{H}} = \frac{E\left\{|d_0|^2\right\}}{E\left\{\left|\kappa^2\sum_{i=0}^{N-1}\sum_{j=0}^{N-1} w_i(j)\Delta_i\right|^2\right\}}. \tag{29}$$

Since $E\{w_i(j)w_v^*(k)\} = 0$ for $j \neq k$ or $i \neq v$, the denominator of (29) can be simplified as follows,

$$\begin{aligned} &E\left\{\left|\kappa^2\sum_{i=0}^{N-1}\sum_{j=0}^{N-1} w_i(j)\Delta_i\right|^2\right\} \\ &= \kappa^4\sum_{i=0}^{N-1}\sum_{i'=0}^{N-1}\Delta_i\Delta_{i'}^*\sum_{j=0}^{N-1}\sum_{j'=0}^{N-1}E\{w_i(j)w_{i'}^*(j')\} \\ &= \kappa^2\sigma_w^2\sum_{i=0}^{N-1}|\Delta_i|^2. \end{aligned} \tag{30}$$

It is worth noting that (30) can be obtained using Parseval's theorem as well,

$$E\left\{\left|\sigma_w^2\sum_{i=0}^{N-1}\sum_{j=0}^{N-1} z_i(j)\Delta_i\right|^2\right\} = \kappa^2\sigma_w^2\sum_{k=0}^{N-1}\frac{1}{|H_k|^2}. \tag{31}$$

Therefore, the SNR using a ZF equalizer is given by

$$\mathrm{SNR}\,|_{\mathbf{H}} = \frac{\sigma_d^2}{\kappa^2\sigma_w^2\sum_{k=0}^{N-1}\frac{1}{|H_k|^2}} \tag{32}$$

where $E\left\{|d_0|^2\right\} = \sigma_d^2$. By denoting $\varphi^{-1} = \kappa^2\sum_{k=0}^{N-1}\frac{1}{|H_k|^2}$, then

$$\mathrm{SNR}\,|_{\mathbf{H}} = \frac{\gamma}{\varphi^{-1}} = \varphi\gamma \tag{33}$$

where $\varphi^{-1} = 1/\varphi$ and $\gamma = \sigma_d^2/\sigma_w^2$. It is interesting to note that (32) and [1, Eq. (61)] are identical, and (32) is similar to [34, Eq. 17] where the block length $M = N$, [9, Eq. 24] for the case of $L_i = 1$, and with [42, Eq. 2] for $t_{k,i} = 1$. Furthermore, it can be noted from (32) that if any subcarrier goes through a deep fade, *i.e.* $\exists k, |H_k|^2 \to 0$, then $1/|H_k|^2 \to \infty$, and hence SNR$\to 0$. Therefore, ZF equalizer is expected to offer poor BER in frequency-selective fading channels even without IN.

Given that the PDF $f_\varphi(\varphi)$ is known, the BER can be expressed as

$$P_{ZF}(\gamma) = \int_0^\infty Q\left(\sqrt{\varphi\gamma}\right) f_\varphi(\varphi)\, d\varphi. \tag{34}$$

Note that φ is composed of the sum of N correlated random variables each of which has the form $|H_k|^{-2}$. If the channel frequency response parameters $\{H_0,..., H_{N-1}\}$ are i.i.d. RV, then evaluating $f_\varphi(\varphi)$ might be feasible for particular scenarios. For example, if we assume that $H_i \sim \mathcal{N}_c(0,1)$, then $|H_i|^2$ has a Chi-square χ^2 PDF with two degrees of freedom, and $|H_i|^{-2}$ has an inverse-χ^2 PDF. Since the inverseχ^2 PDF can be expressed in terms of the inverse Gamma PDF, the PDF of the sum $\sum_i |H_i|^{-2}$ can be evaluated as described in [33]. However, since H_k are correlated, evaluating $f_\varphi(\varphi)$

analytically is difficult. Hence, semi-analytical solutions can be incorporated [9], [34], [42]. In addition, the work of Wang and Giannakis [35] states that systems with instantaneous SNR similar to (33) will not have diversity gain if $\lim_{\gamma \to 0^+} f_\varphi(\varphi) = c > 0$. Moreover, McCloud [34] demonstrated that $f_\varphi(\varphi)$ is bounded away from zero as $\varphi \to 0^+$. This result proves that the proposed interleaved system with ZF equalizer has no diversity gain. Nevertheless, it provides a BER advantage in high SNRs that is very challenging to quantify analytically. Consequently, Monte-Carlo simulations can be invoked to evaluate the system performance. Besides, it can be clearly noticed from (32) that $\mathrm{SNR}\,|_{\mathbf{H}} \to 0$ if any of the subcarriers goes into a deep fade.

B. Samples Blanked, $\epsilon > 0$

In the process of OFDM symbol blanking, a sequence of blanked and non-blanked symbols is generated. Therefore, the input of the deinterleaver can be written as

$$\breve{\mathbf{s}}(\ell) = \begin{cases} 0 \times \breve{\mathbf{y}}(\ell), & \text{blanked symbol} \\ \breve{\mathbf{x}}(\ell) + \breve{\mathbf{\Phi}}(\ell), & \text{otherwise} \end{cases}$$

where $\breve{\mathbf{\Phi}}(\ell)$ is defined in (23). The deinterleaving process rearranges the N OFDM symbols back to their original order before interleaving, which yields $\mathbf{s}(\ell) = \mathbb{B}\mathbf{F}^H\mathbf{d}(\ell) + \mathbb{B}\mathbf{\Phi}(\ell)$, where $\mathbb{B}$ is a matrix that specifies the blanking process. If no symbol is blanked, then $\mathbb{B}$ is the identity matrix. Each of the samples to be blanked is nulled by setting the corresponding main diagonal element to zero. The received signal is then achieved by computing the FFT of $\mathbf{s}$,

$$\mathbf{r}(\ell) = \mathbf{F}\mathbb{B}\mathbf{F}^H\mathbf{d}(\ell) + \mathbf{F}\mathbb{B}\mathbf{\Phi}(\ell). \tag{35}$$

Using the Appendix A, the first term in (35), $\mathbf{v} \triangleq \mathbf{F}\mathbb{B}\mathbf{F}^H\mathbf{d}(\ell)$ can be calculated for a particular $\mathbb{B}$. Thus, the kth sample of $\mathbf{v}$ is given by,

$$v_k(\ell|\epsilon) = \beta d_k + \kappa^2 \sum_{\substack{i=0 \\ i\neq k}}^{N-1} d_i \frac{\sin\left[\pi\epsilon\kappa^2(k-i)\right]}{\sin\left[\pi\kappa^2(i-k)\right]} \mathrm{e}^{-j\frac{\pi}{N}(\epsilon+1)(i-k)} \tag{36}$$

where $\beta = \frac{N-\epsilon}{N}$ and $\epsilon = N - \mathrm{tr}(\mathbb{B})$ represents the number of blanked symbols and $\mathrm{tr}(\cdot)$ denotes the trace.

The second term in (35), can be calculated for the $\ell = 0$ case as follows,

$$\mathbf{F}\mathbb{B}\mathbf{\Phi}(0) = \kappa^3 \begin{bmatrix} \sum_{j,i,k=0}^{N-1} b_j \frac{w_i(j)}{H_k(j)} \mathrm{e}^{-\omega(ik+0\ j)} \\ \sum_{j,i,k=0}^{N-1} b_j \frac{w_i(j)}{H_k(j)} \mathrm{e}^{-\omega(ik+j)} \\ \vdots \\ \sum_{j,i,k=0}^{N-1} b_j \frac{w_i(j)}{H_k(j)} \mathrm{e}^{-\omega(ik+Nj)} \end{bmatrix}$$

where $b_j = \mathbb{B}(j,j)$. The assumption that $\ell = 0$ is used for notational simplicity. Following the same approach described in previous subsection we obtain

$$r_k = \beta d_k + \kappa^2 \sum_{\substack{i=0 \\ i\neq k}}^{N-1} d_i \frac{\sin\left[\pi\epsilon\kappa^2(k-i)\right]}{\sin\left[\pi\kappa^2(i-k)\right]} e^{-j\frac{\pi}{N}(\epsilon+1)(i-k)} + \kappa^3 \sum_{j=0}^{N-1} b_j \sum_{i=0}^{N-1} w_i(j) \sum_{k=0}^{N-1} \frac{\mathrm{e}^{-\omega ik}}{H_k(j)} \tag{37}$$

where the second and third terms in (37) represent the ICI and additive noise, respectively. As depicted in the Appendix A, the noise variance is given by

$$\sigma^2_{w\epsilon} = E\left\{ \left| \kappa^3 \sum_{j=0}^{N-1} b_j \sum_{i=0}^{N-1} w_i(j) \sum_{k=0}^{N-1} \frac{\mathrm{e}^{-wik}}{H_k(j)} \right|^2 \right\} = \beta\kappa^2\sigma_w^2 \sum_{k=0}^{N-1} \frac{1}{|H_k|^2} \tag{38}$$

$\sigma^2_{w\epsilon} = \beta^2\sigma_w^2$ represents the variance of the AWGN given that ϵ samples are blanked, and the ICI variance is

$$\sigma^2_{ICI,k} = \kappa^4\sigma_d^2 \sum_{\substack{i=0 \\ i\neq k}}^{N-1} \frac{\sin^2\left[\pi\epsilon\kappa^2(k-i)\right]}{\sin^2\left[\pi\kappa^2(i-k)\right]}. \tag{39}$$

Therefore, the SINR for the kth subcarrier can be calculated as

$$\mathrm{SINR}\,|_{\mathbf{H},\epsilon,k} = \beta^2 \frac{\sigma_d^2}{\sigma^2_{w\epsilon} + \sigma^2_{ICI,k}}. \tag{40}$$

Since all subcarriers will experience the same SINR, the subcarrier index k can be set to zero and dropped from (41) without loss of generality. Substituting (39) into (41) and simplifying the results gives

$$\mathrm{SINR}\,|_{\mathbf{H},\epsilon} = \left[\frac{\kappa^2}{\gamma} \sum_{i=0}^{N-1} \frac{1}{|H_i|^2} + \frac{\kappa^4}{\beta^2} \sum_{i=1}^{N-1} \frac{\sin^2\left(\pi\epsilon\kappa^2 i\right)}{\sin^2\left(\pi\kappa^2 i\right)} \right]^{-1}. \tag{41}$$

The BER can be calculated by substituting (41) into the well known QPSK error formula,

$$P(e|\epsilon,\mathbf{H}) = Q\left(\sqrt{\mathrm{SINR}\,|_{\mathbf{H},\epsilon}}\right). \tag{42}$$

Therefore,

$$P(e|\mathbf{H}) = \sum_{\epsilon=0}^{N-1} Q\left(\sqrt{\mathrm{SINR}\,|_{\mathbf{H},\epsilon}}\right) \binom{N}{i} p^\epsilon (1-p)^{N-\epsilon}. \tag{43}$$

The conditional BER given in (41) can be used to compute the average BER semi-analytically by generating a large number of realizations for $\mathbf{H}$.

VI. System Performance in Fading Channels (MMSE)

A. No Samples are Blanked, $\epsilon = 0$

The typical approach to mitigate the performance degradation of ZF equalizers is to use MMSE equalizers, where the output signal of such equalizers can be calculated as $\breve{\mathbf{s}} = \left[\mathbb{H}^*\mathbb{H} + \xi\mathbf{I}\right]^{-1}\mathbb{H}^*\breve{\mathbf{y}}$, where $\xi = \gamma^{-1}$ for optimum error performance. Considering that fact that $\mathbb{H} = \mathbf{F}^H\mathbf{H}\mathbf{F}$ and noting that the input samples to the equalizer are interleaved, the equalizer output can be written as

$$\breve{\mathbf{s}} = \mathbf{F}^H\left[\mathbf{H}^*\mathbf{H} + \xi\mathbf{I}\right]^{-1}\mathbf{H}^*\mathbf{F}\breve{\mathbf{y}}. \tag{44}$$

By noting that $\breve{\mathbf{y}} = \mathbf{F}^H\mathbf{H}\mathbf{F}\breve{\mathbf{x}} + w$, then (44) is simplified to

$$\breve{\mathbf{s}} = \mathbf{F}^H\left[|\mathbf{H}|^2 + \xi\mathbf{I}\right]^{-1}|\mathbf{H}|^2\mathbf{F}\breve{\mathbf{x}} + \mathbf{F}^H\left[|\mathbf{H}|^2 + \xi\mathbf{I}\right]^{-1}\mathbf{H}^*\mathbf{F}\mathbf{w}. \tag{45}$$

Because $\mathbf{H}$, $\left[|\mathbf{H}|^2 + \xi\mathbf{I}\right]^{-1}|\mathbf{H}|^2 \triangleq \mathbf{\lambda}$ and $\left[|\mathbf{H}|^2 + \xi\mathbf{I}\right]^{-1}\mathbf{H}^* \triangleq \bar{\mathbf{\lambda}}$ are all $N \times N$ diagonal matrices, the equalizer output $\breve{\mathbf{s}}$ can

be written as

$$\check{\mathbf{s}} = \mathbf{F}^H \boldsymbol{\lambda} \mathbf{F} \check{\mathbf{x}} + \mathbf{F}^H \bar{\boldsymbol{\lambda}} \mathbf{F} \mathbf{w} \tag{46}$$

where

$$\lambda_k = \frac{|H_k|^2}{|H_k|^2 + \xi}, \quad \bar{\lambda}_k = \frac{H_k^*}{|H_k|^2 + \xi} \tag{47}$$

It is clear that when $\xi = 0$, then $\mathbf{F}^H \boldsymbol{\lambda} \mathbf{F} = \mathbf{I}_N$ and $\mathbf{F}^H \bar{\boldsymbol{\lambda}} \mathbf{F} = \mathbf{H}^{-1}$, which implies that the MMSE equalizer becomes ZF equalizer. For $\xi > 0$, $\check{\mathbf{s}}$ will have some sort of inter-symbol interference (ISI) because $\mathbb{A}$ is not a diagonal matrix. Consequently, a compromise has to be made between the degradation resulted from the ISI and noise-enhancement problem. Obviously, setting $\xi = 1/\gamma$ yields the conventional MMSE equalizer, which is widely used in the literature [36].

The FFT output for the proposed system can be derived using Appendix B. The kth sample of the FFT output is given by

$$\begin{aligned} r_k(\ell) &= \kappa^2 \sum_{m=0}^{N-1} \sum_{i=0}^{N-1} x_m(i) \Lambda_{\langle i-\ell \rangle} \mathrm{e}^{-\omega k m} \\ &\quad + \kappa^2 \sum_{m=0}^{N-1} \sum_{i=0}^{N-1} w_i(m) \bar{\Lambda}_{\langle i-\ell \rangle} \mathrm{e}^{-\omega k m} \\ &= \kappa \sum_{i=0}^{N-1} \Lambda_{\langle i-\ell \rangle} d_k(i) + \kappa^2 \sum_{i=0}^{N-1} \sum_{m=0}^{N-1} \bar{\Lambda}_{\langle i-\ell \rangle} w_i(m) \mathrm{e}^{-\omega k m}. \end{aligned} \tag{48}$$

Since all the elements of $\mathbf{r}$ are identically distributed, for simplicity, we consider the first FFT-pin output of the first OFDM symbol,

$$r_0(0) = \kappa d_0(0) \Lambda_0 + \kappa \sum_{i=1}^{N-1} \Lambda_i d_0(i) + \kappa^2 \sum_{i=0}^{N-1} \sum_{m=0}^{N-1} \bar{\Lambda}_i w_i(m). \tag{49}$$

The first term in (49) shows the desired information symbol, whereas the ISI is characterized by the second term and finally, the third term gives the noise component of the received signal. The SINR for a given channel matrix can be expressed as

$$\begin{aligned} \mathrm{SINR}\,|_{\mathbf{H},k=0} &= E\left\{ \left| \kappa d_0(0) \Lambda_0 \right|^2 \right\} \\ &\times \left(E\left\{ \left| \kappa \sum_{i=1}^{N-1} \Lambda_i d_0(i) + \kappa^2 \sum_{i=0}^{N-1} \sum_{m=0}^{N-1} \bar{\Lambda}_i w_i(m) \right|^2 \right\} \right)^{-1}. \end{aligned} \tag{50}$$

Since the noise and ISI terms are independent, it is possible to separate the denominator terms and rewrite (50) as

$$\begin{aligned} \mathrm{SINR}\,|_{\mathbf{H},k=0} &= E\left\{ \left| \kappa d_0(0) \Lambda_0 \right|^2 \right\} \\ &\div \left(E\left\{ \left| \kappa \sum\nolimits_{i=1}^{N-1} \Lambda_i d_0(i) \right|^2 \right\} \right. \\ &\left. + E\left\{ \left| \kappa^2 \sum\nolimits_{i=0}^{N-1} \sum\nolimits_{m=0}^{N-1} \bar{\Lambda}_i w_i(m) \right|^2 \right\} \right). \end{aligned} \tag{51}$$

The expected value of the desired signal can be reduced to

$$\begin{aligned} E\left\{ \left| \kappa d_0(0) \Lambda_0 \right|^2 \right\} &= \kappa^2 E\left\{ \left| d_0(0) \right|^2 \right\} \left| \Lambda_0 \right|^2 \\ &= \kappa^2 \sigma_d^2 \left| \Lambda_0 \right|^2. \end{aligned} \tag{52}$$

The denominator of (51) is composed of two parts, $\digamma_1$ and $\digamma_2$. Since $E\{d_0(i) d_0(i')\} = 0$ for $i \neq i'$, and $E\left\{ |d_0(i)|^2 \right\} = \sigma_d^2$, then $\digamma_1$ and $\digamma_2$ are reduced to,

$$\digamma_1 \triangleq E\left\{ \left| \kappa \sum_{i=1}^{N-1} \Lambda_i d_0(i) \right|^2 \right\} = \kappa^2 \sigma_d^2 \sum_{i=1}^{N-1} |\Lambda_i|^2. \tag{53}$$

And similarly,

$$\digamma_2 \triangleq \kappa^4 E\left\{ \left| \sum_{i=0}^{N-1} \sum_{m=0}^{N-1} \bar{\Lambda}_i w_i(m) \right|^2 \right\} = \kappa^2 \sigma_w^2 \sum_{i=0}^{N-1} \left| \bar{\Lambda}_i \right|^2. \tag{54}$$

Following the same approach used for the ZF equalizer, and inserting (53) and (54) into (51) gives

$$\mathrm{SINR}\,|_{\mathbf{H},k=0} = \frac{\sigma_d^2 \left| \Lambda_0 \right|^2}{\sigma_d^2 \sum_{i=1}^{N-1} |\Lambda_i|^2 + \sigma_w^2 \sum_{i=0}^{N-1} \left| \bar{\Lambda}_i \right|^2}. \tag{55}$$

By substituting the values of Λ_0, Λ_i and $\bar{\Lambda}_i$ into (55), using the fact that $\sum_{i=0}^{N-1} \frac{\mathrm{e}^{-\omega i(k-n)}}{H_k H_n^*} = 0$, $\forall\ k \neq n$, and noting that all subcarriers will experience the same SINR, then SINR at the FFT output can be expressed as

$$\mathrm{SINR}\,|_{\mathbf{H}} = \gamma \frac{\sum_{k=0}^{N-1} \lambda_k}{\sum_{k=0}^{N-1} \frac{\lambda_k}{|H_k|^2}}. \tag{56}$$

The SINR given in (56) is equal to SINR of the WHT-OFDM system [9], [1, Eq. (68)]. Consequently, the two systems will have equal BER in fading channels. The BER of the proposed system with MMSE can be calculated semi-analytically as

$$P_{MMSE}(\gamma) = \frac{1}{L} \sum_{i=1}^{L} Q\left(\sqrt{\mathrm{SINR}\,|_{\mathbf{H}_i}} \right) \tag{57}$$

where $\mathbf{H}_i$ is the ith realization of $\mathbf{H}$ and L is the total number of realizations**.**

From the definition of λ_k (47), it is evident that unless the subcarrier k is in deep fade, λ is very close to 1. Thus, the summation $\gamma \sum_{k=0}^{N-1} \lambda_k$ in (56) is generally comparable to $\frac{\sigma_d^2}{\kappa^2 \sigma_w^2} = N\gamma$ in (32). On the other hand, the denominator in (32) is dominated by the subcarriers in the deep fade. *i.e.*, if any of the subcarriers $H_k \longrightarrow 0$, the summation $\sum_{k=0}^{N-1} \frac{1}{|H_k|^2} \to \infty$, resulting in very low SNR. This effect has been evaded in MMSE since $\sum_{k=0}^{N-1} \frac{\lambda_k}{|H_k|^2}$ is bounded away from infinity. This leads to substantially higher SNR than TDI with ZF equalizer and diversity advantages in the operational SNRs [37].

B. Samples Blanked, $\epsilon > 0$

Similar to the ZF case, some OFDM symbols are blanked if they are declared as contaminated by the IN bursts. Therefore, the equalizer output can be written as

$$\check{\mathbf{s}}(\ell) = \begin{cases} 0 \times \check{\mathbf{y}}, & \text{blanked symbol} \\ \check{\boldsymbol{\Theta}}(\ell) + \check{\boldsymbol{\Psi}}(\ell), & \text{otherwise} \end{cases} \tag{58}$$

where $\check{\boldsymbol{\Theta}}$ and $\check{\boldsymbol{\Psi}}$ are defined in (83), and (81), respectively. The deinterleaver output $\mathbf{s}(\ell) = \mathbb{B}\boldsymbol{\Theta}(\ell) + \mathbb{B}\boldsymbol{\Psi}(\ell)$ and the FFT output $\mathbf{r}(\ell) = \mathbf{F}\mathbf{s}(\ell) = \mathbf{F}\mathbb{B}\boldsymbol{\Theta}(\ell) + \mathbf{F}\mathbb{B}\boldsymbol{\Psi}(\ell)$, where

$$r_k(\ell) = \underbrace{\kappa^2 \sum_{n=0}^{N-1} b_n \sum_{i=0}^{N-1} x_n(i) \Lambda_{\langle i-\ell \rangle_N} \mathrm{e}^{-\omega n k}}_{v_k(\ell)}$$

$$+\underbrace{\kappa^2\sum_{n=0}^{N-1}b_n\sum_{i=0}^{N-1}w_i(n)\bar{\Lambda}_{\langle i-\ell\rangle_N}\mathrm{e}^{-\omega nk}}_{u_k(\ell)}. \quad (59)$$

The first term in (59) $v_k(\ell)$ can be written as

$$\begin{aligned}v_k(\ell)&=\kappa^2\sum\nolimits_{i=0}^{N-1}\Lambda_{\langle i-\ell\rangle_N}\sum\nolimits_{n=0}^{N-1}b_nx_n(i)\mathrm{e}^{-\omega nk}\\&=\kappa\sum\nolimits_{i=0}^{N-1}\Lambda_{\langle i-\ell\rangle_N}\Bigg(\beta\ d_k(i)\\&\quad+\kappa^2\sum\nolimits_{\substack{n=0\\n\neq k}}^{N-1}d_n(i)\frac{\sin\left[\pi\epsilon\kappa^2(k-n)\right]}{\sin\left[\pi\kappa^2(n-k)\right]}e^{-\frac{\omega}{2}(\epsilon+1)(n-k)}\Bigg).\end{aligned} \quad (60)$$

To simplify the calculations, we consider $\nu_0(0)$, which is equal to

$$\begin{aligned}\nu_0(0)&=\kappa\beta\Lambda_0d_0(0)+\kappa\beta\sum_{i=1}^{N-1}\Lambda_id_0(i)\\&\quad+\kappa^3\sum_{i=0}^{N-1}\Lambda_i\sum_{n=1}^{N-1}d_n(i)\frac{\sin\left[\pi\epsilon\kappa^2n\right]}{\sin\left[\pi\kappa^2n\right]}e^{-j\frac{\pi}{N}(\epsilon+1)n}.\end{aligned} \quad (61)$$

In (61), the first term includes the desired signal and the second term is the interference caused by the MMSE equalizer, whose power is denoted as $\sigma^2_{I,MMSE}$. The last term is the interference caused by losing the blanked ϵ samples from the OFDM symbol, which has a power of $\sigma^2_{I,Blank}$. The equalization and blanking interference power can be calculated as

$$\begin{aligned}\sigma^2_{I,MMSE}&=E\left\{\left|\kappa\beta\sum_{i=1}^{N-1}\Lambda_id_0(i)\right|^2\right\}\\&=\kappa^2\beta^2\sigma_d^2\sum_{i=1}^{N-1}|\Lambda_i|^2.\end{aligned} \quad (62)$$

and

$$\begin{aligned}\sigma^2_{I,Blank}&=E\left\{\left|\kappa^3\sum_{i=0}^{N-1}\Lambda_i\sum_{k=1}^{N-1}d_k(i)\right.\right.\\&\quad\left.\left.\times\frac{\sin\left[\pi\epsilon\kappa^2k\right]}{\sin\left[\pi\kappa^2k\right]}e^{-\frac{\omega}{2}(\epsilon+1)k}\right|^2\right\}\\&=\kappa^6\sigma_d^2\alpha_\epsilon\sum\nolimits_{i=0}^{N-1}|\Lambda_i|^2,\end{aligned} \quad (63)$$

where $\alpha_\epsilon\triangleq\sum_{k=1}^{N-1}\frac{\sin^2(\pi\epsilon\kappa^2k)}{\sin^2(\pi\kappa^2k)}$. The second term in (59), $u_k(\ell)$, describes the noise component of the received signal,

$$\begin{aligned}u_k(\ell)&=\kappa^2\sum_{n=0}^{N-1}b_n\sum_{i=0}^{N-1}w_i(n)\bar{\Lambda}_{\langle i-\ell\rangle_N}\mathrm{e}^{-\omega nk}\\&=\kappa^2\sum_{i=0}^{N-1}\bar{\Lambda}_{\langle i-\ell\rangle_N}\sum_{n=0}^{N-1}b_nw_i(n)\mathrm{e}^{-\omega nk}.\end{aligned}$$

The variance of the noise component is

$$\begin{aligned}\sigma^2_{u\epsilon}&=E\left\{\left|\kappa^2\sum_{i=0}^{N-1}\bar{\Lambda}_{\langle i-\ell\rangle_N}\sum_{n=0}^{N-1}b_nw_i(n)\mathrm{e}^{-\omega nk}\right|^2\right\}\\&=\kappa^2\sigma^2_{w\epsilon}\sum_{i=0}^{N-1}\left|\bar{\Lambda}_i\right|^2.\end{aligned} \quad (64)$$

Note that the second summation in (64) is just the FFT of the noise samples with ϵ samples missing. Consequently, the conditional SINR is calculated as

$$\mathrm{SINR}\,|_{\mathbf{H},\epsilon}=\kappa^2\beta^2\frac{\Lambda_0^2\sigma_d^2}{\sigma^2_{w\epsilon}+\sigma^2_{I,MMSE}+\sigma^2_{I,Blank}}. \quad (65)$$

After some mathematical manipulations (65) can be written as

$$\mathrm{SINR}\,|_{\mathbf{H},\epsilon}=\frac{\sum_k\lambda_k}{\frac{1}{\gamma}\sum_k\frac{\lambda_k}{|H_k|^2}+\frac{\kappa^2}{\beta^2}\alpha_\epsilon\frac{\sum_k\lambda_k^2}{\sum_k\lambda_k}},\quad k=0,1,...N-1. \quad (66)$$

The BER can be computed semi-analytically as described in (43).

In practical OFDM systems, accurate channel estimation, symbol timing and frequency synchronization are necessary to detect the information symbols. Therefore, every transmitted data frame is usually preceded by a preamble of a few OFDM training symbols. Moreover, some subcarriers are also reserved as pilots to assist channel estimation and synchronization. The number and distribution of the pilots depend on the nature of the channel [3], [4]. For the TDI, the received signal described in (20) clearly implies that the channel matrix $\mathbf{H}$ should be estimated and compensated before the deinterleaving process. Consequently, if typical channel estimation and synchronization techniques are to be used, the training OFDM symbols within the frame preamble should not be interleaved. Moreover, for various OFDM systems that does not involve mobility such as PLC, the channel can be considered relatively fixed for the entire frame period [43]. If the channel or synchronization parameters need to be updated more frequently, then time-domain [44] or blind techniques can be invoked [45].

VII. Numerical Results

Monte Carlo simulations are used to evaluate the performance of the proposed system over frequency-selective multipath fading channels. The OFDM system considered in this paper has $N=128$ and $\bar{N}=16$. All data symbols are QPSK modulated. The channel is assumed to be time-invariant throughout the duration of each interleaving block. In addition, full channel state information and perfect synchronization are assumed throughout this work. Each simulation run consists of 2.56×10^6 independent OFDM symbols. The multipath fading channel model considered in this work corresponds to a Rayleigh frequency-selective channel with normalized delays of [0, 1, 2, 3, 4] samples and average gains [0.35, 0.25, 0.18, 0.12, 0.1]. The IN is modeled as GBG process, where the bursts position is uniformly distributed within the OFDM symbol period. Unless it is specified otherwise, the burst gating factor probability $p=0.01$, the burst width $\varkappa=(N+\bar{N})/2$, the signal-to-IN ratio SIR $=-20$ dB and SNR $\triangleq\gamma$.

To demonstrate the effect of TDI on the decision variables $\mathbf{r}$ at the FFT output, the magnitude of the noise term in each subcarrier is presented for a particular channel realization as shown in Fig. 2. The aggregate noise and interference (AGNI) output at the kth subcarrier is computed as $|r_k-d_k|^2$. The AGNI is selected because it clearly reveals the noise

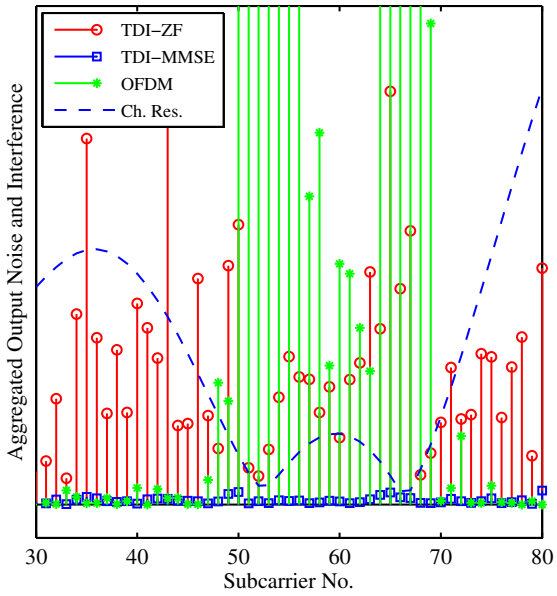

Fig. 2. Noise enhancement of the TDI and OFDM systems with ZF and MMSE equalizers for $SNR = 15$ dB.

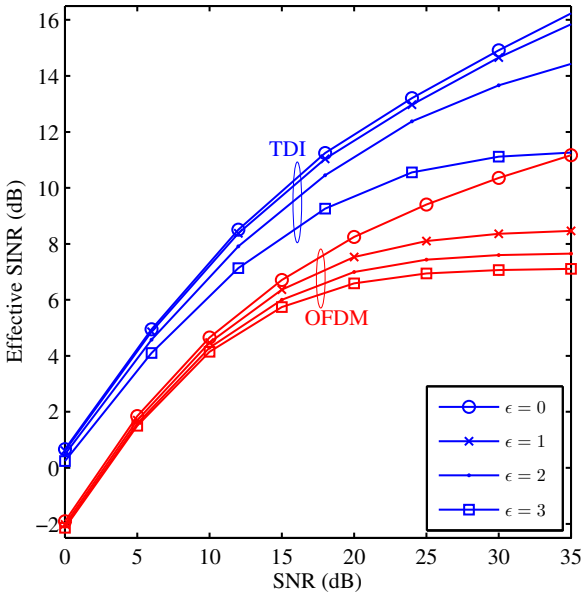

Fig. 3. Effective SINR of TDI and OFDM for different values of ϵ.

enhancement problem caused by the ZF equalizer. As it can be observed from the figure, the channel has two nulls at subcarriers 50 to 56 and 64 to 69. As expected, the division by the relevant H_k in conventional OFDM will cause severe noise enhancement for the subcarriers with deep fading as shown in Fig. 2. The ZF equalizer and the last FFT mixes the channel frequency response (CFR) of all subcarriers, which mainly will deteriorate the BER performance as the enhanced noise is distributed over all subcarriers. Finally, the MMSE does not suffer from any noticeable noise enhancement problem due to the bias added to H_k before the division process, which proves that the CFR mixing process is advantageous and will cause BER improvement.

Fig. 3 presents the effective SINR of the TDI and OFDM systems versus the SNR γ, which measures the SNR degradation caused by both, fading and blanking. The immunity of the TDI to fading can be observed from the $\epsilon = 0$ case where the SINR of the TDI is about 5 dB higher than the conventional OFDM. It is evident that OFDM suffers from losing some samples, where $\epsilon > 0$, more than TDI which leads to the increase in the SINR gap to approximately 7 and 7.5 dB for $\epsilon = 2$ and 1, respectively. For $\epsilon \geq 3$, the effective SINR becomes very low, which decreases the SINR difference to about 4 dB. In other words, despite OFDM that is degraded even with $\epsilon = 1$, TDI can successfully resist the adverse effect of losing samples up to $\epsilon = 3$, where its slope becomes equal to that of OFDM.

The BER performance of IN-free ($\epsilon = 0$) TDI, WHT-OFDM and conventional OFDM systems using ZF and MMSE equalizers is given in Fig. 4. As it can be noted from the figure, the lowest BER is achieved by the TDI/WHT using MMSE, whereas the TDI/WHT ZF gives the worst BER. The OFDM inherent fading-resistance gives it a mediocre performance. Since OFDM transmits the signal in orthogonal narrow frequency band channels, both equalizers give the same

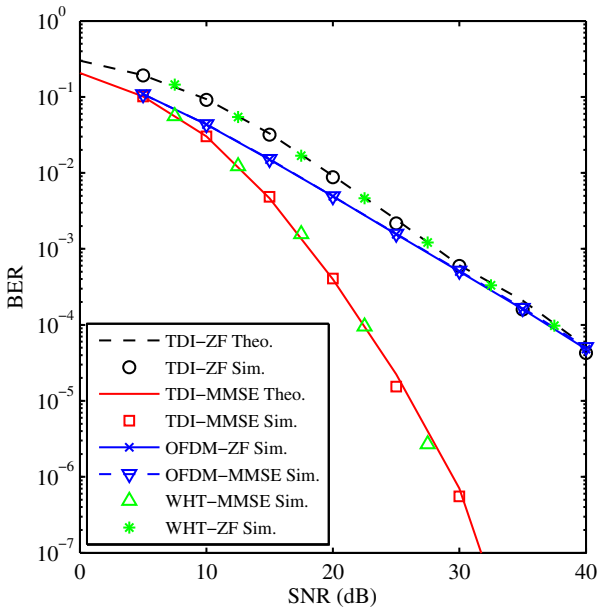

Fig. 4. BER of the TDI and conventional OFDM using ZF and MMSE equalizers.

BER; a result which is expected. Moreover, the simulation results in this figure corroborate with the analysis. In addition, the BER curves of WHT-OFDM with MMSE and TDI-MMSE match, which indicates that TDI-MMSE and WHT-OFDM using MMSE provide equal diversity advantages. As expected, the ZF suffers from noise enhancement problem which can be observed in all ZF equalizers.

Fig. 5 shows the BER versus $\mathcal{T}_1$ using different values of $\mathcal{T}_2$ and SNR. It can be noted from the figure that there is no unique optimum ($\mathcal{T}_1$, $\mathcal{T}_2$) that should be used. Moreover, once $\mathcal{T}_2$ is selected, $\mathcal{T}_1$ can be selected without a major concern about its accuracy due to the BER plateau shown in Fig. 5. Therefore, the thresholds selection process is relaxed

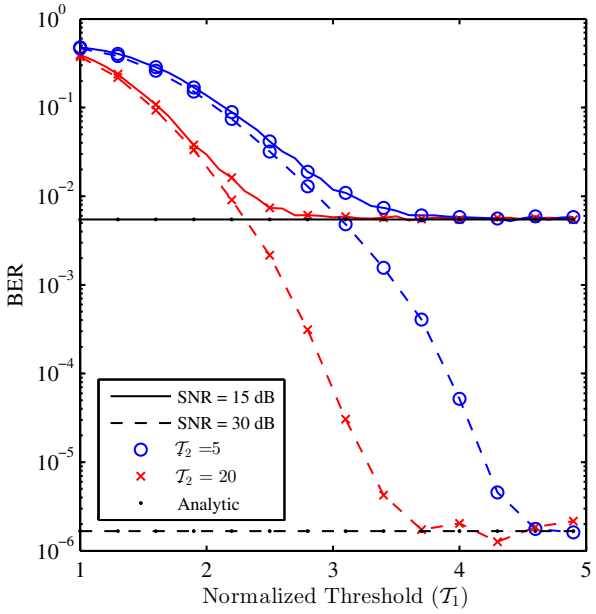

Fig. 5. BER versus the threshold $\mathcal{T}_1$ for different values of $\mathcal{T}_2$ and SNR.

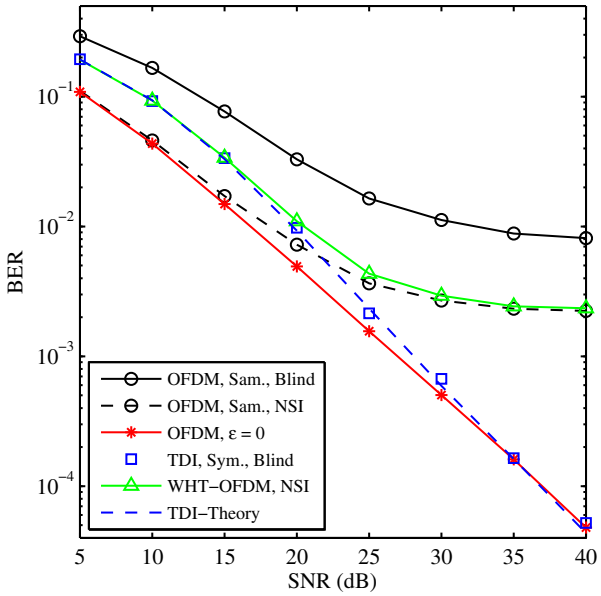

Fig. 6. BER using ZF equalizer in the presence of IN.

as compared to the sample-by-sample blanking. Besides, it is interesting to note that analytical BER can be achieved regardless of the SNR.

Fig. 6 shows the joint effect of IN and fading, and compares the BER of TDI, OFDM and WHT-OFDM using ZF equalization. The performance of OFDM without IN is shown in the figure as the baseline. The blind blanking is performed by comparing the received sample to the optimum thresholds, while non-blind is performed by assuming that the receiver has perfect IN state information (NSI). In general, OFDM systems offer poor performance in IN channels even when blanking is invoked and the perfect NSI is available. The simulation results show that OFDM exhibits an error floor greater than 10^{-3}, which persists even with NSI. Similar to the conventional OFDM, the WHT-OFDM system does not offer any noticeable immunity against IN. Although the TDI-ZF does not offer BER improvement in frequency-selective fading channels, it managed to mitigate the IN reasonably, where the BER converges to the OFDM BER with $\epsilon = 0$. Furthermore, the BER of blind symbol blanking applied for TDI matches the BER of ideal blanking with NSI. In all other cases, a severe BER degradation is observed.

The BER of TDI-MMSE is compared to OFDM and WHT-OFDM in Fig. 7, where the results clearly show that the TDI significantly outperforms the other considered systems. In addition to the high robustness in frequency-selective fading channels, the TDI can effectively combat the degradation caused by IN bursts with less than 1 dB degradation from the IN-free case at BER of 10^{-6}. Both, the OFDM and WHT-OFDM exhibit high errors at SNR of about 35 dB. However, the WHT-OFDM slightly outperforms the conventional OFDM due to its robustness to fading. Comparing the BER for the blind and NSI blanking in TDI shows that blind symbol blanking can be performed with high accuracy. This figure also shows the agreement between semi-analytical and simulation results.

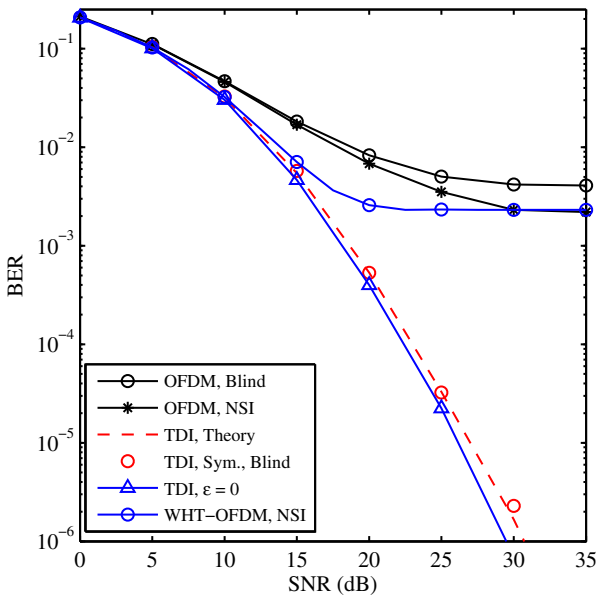

Fig. 7. BER using MMSE equalizer in the presence of IN.

The effect of the IN bursts arrival probability is given in Fig. 8. It can be noted from the figure that the TDI BER degradation for $p \lesssim 0.02$ is negligible, while an error floor is observed at $BER \approx 10^{-4}$ for $p = 0.05$. It is worth noting that $P(\epsilon \geq 1)|_{p=0.02} \approx 0.92$, which corresponds to a severe IN channel where every block of N OFDM symbols will be mainly hit by one or more IN bursts. For the $p = 0.05$ and 0.1 cases, $P(\epsilon \geq 3)|_{p=0.05} \approx 0.96$ and $P(\epsilon \geq 3)|_{p=0.1} \approx 1$, respectively. Therefore, the TDI can offer a superior BER performance even in severe IN channels where $p = 0.05$. The $p = 0.1$ case is too extreme, and hence it will be difficult to have reliable communications in such scenarios.

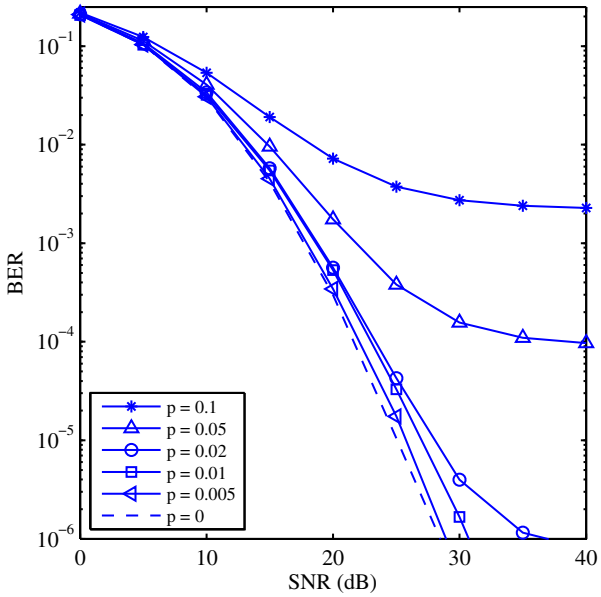

Fig. 8. BER of the TDI for different gating probability p.

VIII. Conclusion

This work presented a novel technique for joint mitigation of impulsive noise (IN) and multipath fading effects in broadband communication systems with OFDM modulation. The proposed system, namely TDI, is composed of the time domain interleaving that interleaves the samples of several OFDM symbols after the IFFT and deinterleaves them before the final FFT stage, and a two-stage blanking to mitigate the IN. The performance of the TDI in presence of IN has been analyzed in multipath fading channels where ZF and MMSE equalizers are employed to compensate the frequency-selectivity effects. The performance of the proposed system is evaluated in terms of BER where closed-form formulae are derived for the SINR using ZF and MMSE equalizers. The obtained analytical and simulation results show that the TDI can effectively combat the effects of heavily distributed IN and the frequency-selectivity of the channel. Our analyses show that the effective SINR of TDI is mathematically equal to that of Walsh-Hadamard precoded OFDM (WHT-OFDM) system, which proves that equal frequency diversity gain is obtained [1]. Moreover, the TDI has time diversity, which was effectively used to reduce the BER degradation caused by the IN.

Appendix A
The Disturbance Caused by Blanking

Assume that $\mathbf{x} = \mathcal{F}^{-1}\{\mathbf{d}\}$. Therefore,

$$x_n = \kappa \sum_{i=0}^{N-1} d_i e^{\omega i n}. \tag{67}$$

Given that ϵ samples of $\mathbf{x}$ are zeroed, calculating $\mathbf{s} = \mathcal{F}\{\mathbf{y}\}$, where $\mathbf{y} = \mathbb{B}\mathbf{x}$, gives

$$s_k|\epsilon = \kappa \sum_{n=0}^{N-1} y_n e^{-\omega n k} = \kappa \sum_{n=\epsilon}^{N-1} x_n e^{-\omega n k} \tag{68}$$

Inserting (68) in (67), gives

$$\begin{aligned} s_k|\epsilon &= \kappa^2 \sum_{n=\epsilon}^{N-1} \sum_{i=0}^{N-1} d_i e^{\omega i n} e^{-\omega n k} \\ &= \beta d_k + \kappa^2 \sum_{n=\epsilon}^{N-1} \sum_{\substack{i=0 \\ i\neq k}}^{N-1} d_i e^{\omega n (i-k)} \end{aligned} \tag{69}$$

where $\beta = \frac{N-\epsilon}{N}$. With the change of the summations order, it can be rewritten as

$$= \beta d_k + \kappa^2 \sum_{\substack{i=0 \\ i\neq k}}^{N-1} d_i \sum_{n=\epsilon}^{N-1} e^{\omega n (i-k)}. \tag{70}$$

The last summation can be simplified using the identity

$$\sum_{n=\epsilon}^{N-1} e^{\omega n (i-k)} = \frac{\mathrm{e}^{-2\,j\pi\,(-k-iN+kN)\kappa^2} - \mathrm{e}^{-2\,j\pi\,(-k-\epsilon i+\epsilon k)\kappa^2}}{\mathrm{e}^{2\,j\pi\,i\kappa^2} - \mathrm{e}^{2\,j\pi\,k\kappa^2}}$$

and taking $\mathrm{e}^{\frac{2\,j\pi\,k}{N}}$ as a common factor, which results in

$$\sum_{n=\epsilon}^{N-1} e^{\omega n (i-k)} = \frac{\mathrm{e}^{2\,j\pi(i-k)} - \mathrm{e}^{2\,j\pi\epsilon(i-k)\kappa^2}}{\mathrm{e}^{2\,j\pi(i-k)\kappa^2} - 1}. \tag{71}$$

Note that $\mathrm{e}^{2\,j\pi(i-k)} = 1$. Thus

$$\sum_{n=\epsilon}^{N-1} e^{\omega n (i-k)} = \frac{1 - \mathrm{e}^{2\,j\pi\epsilon(i-k)\kappa^2}}{\mathrm{e}^{2\,j\pi(i-k)\kappa^2} - 1} \tag{72}$$

Using Euler formula, and after some algebraic manipulations, we have

$$1 - \mathrm{e}^{2\,jm} = 2\sin m\,(\sin m - j\cos m)$$

where $m = \frac{\pi\epsilon(i-k)}{N}$. Similarly, letting $\frac{\pi(i-k)}{N} = u$, gives $\mathrm{e}^{2\,ju} - 1 = 2\sin u\,[-\sin u + j\cos u]$. Therefore,

$$\begin{aligned} \sum_{n=\epsilon}^{N-1} e^{\omega n (i-k)} &= \frac{\sin m}{\sin u}\,\frac{\sin m - j\cos m}{-\sin u + j\cos u} \\ &= -\frac{\sin m}{\sin u} e^{-j(m+u)} \\ &= \frac{\sin\left[\pi\epsilon\kappa^2(k-i)\right]}{\sin\left[\pi\kappa^2(i-k)\right]} e^{-j\pi\kappa^2(\epsilon+1)(i-k)} \end{aligned}$$

Finally,

$$s_k|\epsilon = \beta d_k + \kappa^2 \sum_{\substack{i=0 \\ i\neq k}}^{N-1} d_i \frac{\sin\left[\pi\epsilon\kappa^2(k-i)\right]}{\sin\left[\pi\kappa^2(i-k)\right]} e^{-j\pi\kappa^2(\epsilon+1)(i-k)} \tag{73}$$

The second term corresponds with the error caused by zeroing some samples of $\mathbf{x}$ and its mean is

$$E\left\{\kappa^2 \sum_{\substack{i=0 \\ i\neq k}}^{N-1} d_i \frac{\sin\left[\pi\epsilon\kappa^2(k-i)\right]}{\sin\left[\pi\kappa^2(i-k)\right]} e^{-j\pi\kappa^2(\epsilon+1)(i-k)}\right\} = 0. \tag{74}$$

The variance of this error can be computed as

$$\begin{aligned} \sigma_k^2 &= E\left\{\left|\kappa^2 \sum_{\substack{i=0 \\ i\neq k}}^{N-1} d_i \frac{\sin\left[\pi\epsilon\kappa^2(k-i)\right]}{\sin\left[\pi\kappa^2(i-k)\right]} e^{-j\pi\kappa^2(\epsilon+1)(i-k)}\right|^2\right\} \\ &= \kappa^4 E\left\{\sum_{\substack{i=0 \\ i\neq k}}^{N-1} \sum_{\substack{v=0 \\ v\neq k}}^{N-1} E\left\{d_i d_v^*\right\} \frac{\sin\left[\frac{\pi\epsilon}{N}(k-i)\right]}{\sin\left[\frac{\pi}{N}(i-k)\right]}\right. \end{aligned}$$

$$\times \frac{\sin\left[\frac{\pi\epsilon}{N}(k-v)\right]}{\sin\left[\frac{\pi}{N}(v-k)\right]} e^{j\frac{\pi}{N}(\epsilon+1)(v-i)} \Bigg\} \quad (75)$$

Assuming that the data samples d_i are independent and identically distributed with $E\{d_i d_k\} = 0\ \forall i \neq k$ and variance σ_d^2, then

$$\sigma_k^2 = \kappa^4 \sum_{\substack{i=0 \\ i\neq k}}^{N-1} E\{d_i d_i^*\} \frac{\sin\left[\pi\epsilon\kappa^2(k-i)\right]}{\sin\left[\pi\kappa^2(i-k)\right]} \frac{\sin\left[\pi\epsilon\kappa^2(k-i)\right]}{\sin\left[\pi\kappa^2(i-k)\right]}$$

$$= \frac{\sigma_d^2}{N^2} \sum_{\substack{i=0 \\ i\neq k}}^{N-1} \frac{\sin^2\left[\pi\epsilon\kappa^2(k-i)\right]}{\sin^2\left[\pi\kappa^2(i-k)\right]} \quad (76)$$

APPENDIX B
TDI-MMSE PROCESSING

For the case of MMSE equalizer without blanking, the equalizer output $\check{\mathbf{s}}$ can be written as

$$\check{\mathbf{s}} = \mathbf{F}^H \boldsymbol{\lambda} \mathbf{F} \check{\mathbf{x}} + \mathbf{F}^H \bar{\boldsymbol{\lambda}} \mathbf{F} \mathbf{w} \quad (77)$$

where λ_k and $\bar{\lambda}_k$ are defined in (47). Let $\mathbb{A} \triangleq \mathbf{F}^H \boldsymbol{\lambda} \mathbf{F}$ and $\mathbb{A}' \triangleq \mathbf{F}^H \bar{\boldsymbol{\lambda}} \mathbf{F}$ where $\mathbb{A}$ and $\mathbb{A}'$ are circulant matrices with their first rows defined as

$$\mathbb{A}(0,:) = \kappa^2 \begin{bmatrix} \sum_{k=0}^{N-1} \lambda_k \\ \sum_{k=0}^{N-1} \lambda_k e^{-\omega k} \\ \sum_{k=0}^{N-1} \lambda_k e^{-\omega 2k} \\ \vdots \\ \sum_{k=0}^{N-1} \lambda_k e^{-\omega(N-1)k} \end{bmatrix}^T \quad (78)$$

and

$$\mathbb{A}'(0,:) = \kappa^2 \begin{bmatrix} \sum_{k=0}^{N-1} \bar{\lambda}_k \\ \sum_{k=0}^{N-1} \bar{\lambda}_k e^{-\omega k} \\ \sum_{k=0}^{N-1} \bar{\lambda}_k e^{-\omega 2k} \\ \vdots \\ \sum_{k=0}^{N-1} \bar{\lambda}_k e^{-\omega(N-1)k} \end{bmatrix}^T . \quad (79)$$

Thus, the MMSE equalizer output in (46) can be reduced to

$$\check{\mathbf{s}} = \mathbb{A}\check{\mathbf{x}} + \mathbb{A}'\mathbf{w}. \quad (80)$$

Following the same approach used for the ZF equalizer, we define $\check{\boldsymbol{\Psi}} \triangleq \mathbb{A}' w$ similar to $\check{\boldsymbol{\Phi}}$ except that $1/H_k$ is replaced by $\bar{\lambda}_k$. Therefore,

$$\check{\boldsymbol{\Psi}}(\ell) = \kappa^2 \begin{bmatrix} \sum_{i,k=0}^{N-1} w_i(\ell) \bar{\lambda}_k e^{-\omega k\langle i-0\rangle} \\ \sum_{i,k=0}^{N-1} w_i(\ell) \bar{\lambda}_k e^{-\omega k\langle i-1\rangle} \\ \vdots \\ \sum_{i,k=0}^{N-1} w_i(\ell) \bar{\lambda}_k e^{-\omega k\langle i-N+1\rangle} \end{bmatrix} . \quad (81)$$

By denoting $\bar{\Lambda}_i = \kappa \sum_{k=0}^{N-1} \bar{\lambda}_k e^{-\omega k i}$, which is the is the FFT of $\bar{\boldsymbol{\lambda}}$ ($\bar{\boldsymbol{\Lambda}} = \mathcal{F}\{\bar{\boldsymbol{\lambda}}\}$), then (81) can be written as

$$\check{\boldsymbol{\Psi}}(\ell) = \kappa \begin{bmatrix} \sum_{i=0}^{N-1} w_i(\ell) \bar{\Lambda}_i \\ \sum_{i=0}^{N-1} w_i(\ell) \bar{\Lambda}_{\langle i-1\rangle} \\ \vdots \\ \sum_{i=0}^{N-1} w_i(\ell) \bar{\Lambda}_{\langle i-N+1\rangle} \end{bmatrix} . \quad (82)$$

The symbol index ℓ is added in (81) to denote the noise sample taken at ℓth OFDM symbol, which is needed to represent the deinterleaved noise. The first term in (80) can be written as

$$\check{\boldsymbol{\Theta}}(\ell) \triangleq \mathbb{A}\check{\mathbf{x}} = \kappa^2 \begin{bmatrix} \sum_{i,k=0}^{N-1} x_\ell(i) \lambda_k e^{-\omega k\langle i-0\rangle} \\ \sum_{i,k=0}^{N-1} x_\ell(i) \lambda_k e^{-\omega k\langle i-1\rangle_N} \\ \vdots \\ \sum_{i,k=0}^{N-1} x_\ell(i) \lambda_k e^{-\omega k\langle i-N+1\rangle_N} \end{bmatrix}^T . \quad (83)$$

By denoting $\Lambda_i = \kappa \sum_{k=0}^{N-1} \lambda_k e^{-\omega k i}$, which is the FFT of $\boldsymbol{\lambda}$ ($\boldsymbol{\Lambda} = \mathcal{F}\{\boldsymbol{\lambda}\}$), then (83) can be written as

$$\check{\boldsymbol{\Theta}}(\ell) = \kappa \begin{bmatrix} \sum_{i=0}^{N-1} x_\ell(i) \Lambda_{\langle i-0\rangle} \\ \sum_{i=0}^{N-1} x_\ell(i) \Lambda_{\langle i-1\rangle_N} \\ \vdots \\ \sum_{i=0}^{N-1} x_\ell(i) \Lambda_{\langle i-N+1\rangle_N} \end{bmatrix} . \quad (84)$$

The MMSE output is

$$\check{\mathbf{s}}(\ell) = \check{\boldsymbol{\Theta}}(\ell) + \check{\boldsymbol{\Psi}}(\ell), \quad (85)$$

where

$$\check{s}_n(\ell) = \kappa \sum_{i=0}^{N-1} x_\ell(i) \Lambda_{\langle i-n\rangle} + \kappa \sum_{i=0}^{N-1} w_i(\ell) \bar{\Lambda}_{\langle i-n\rangle}. \quad (86)$$

The next step is to deinterleave $\check{\mathbf{s}}(\ell)$, which can be calculated by substituting (81) and (83) into (85). The result is the desired deinterleaved signal $\mathbf{s}(\ell) = \boldsymbol{\Theta}(\ell) + \boldsymbol{\Psi}(\ell)$, where

$$s_n(\ell) = \kappa \sum_{i=0}^{N-1} x_n(i) \Lambda_{\langle i-\ell\rangle} + \kappa \sum_{i=0}^{N-1} w_i(n) \bar{\Lambda}_{\langle i-\ell\rangle}. \quad (87)$$

The final step is to apply the FFT to get the N decision variables $\mathbf{r}(\ell) = \mathbf{F}\mathbf{s}(\ell) = \mathbf{F}\boldsymbol{\Theta}(\ell) + \mathbf{F}\boldsymbol{\Psi}(\ell)$, which are then applied to the demodulator to get the information symbols. After some algebraic manipulations, $\mathbf{F}\boldsymbol{\Theta}(\ell)$ and $\mathbf{F}\boldsymbol{\Psi}(\ell)$ can be written as

$$\mathbf{F}\boldsymbol{\Theta}(\ell) = \kappa^2 \begin{bmatrix} \sum_{m,i=0}^{N-1} x_m(i) \Lambda_{\langle i-\ell\rangle} \\ \sum_{m,i=0}^{N-1} x_m(i) \Lambda_{\langle i-\ell\rangle} e^{-\omega m} \\ \vdots \\ \sum_{m,i=0}^{N-1} x_m(i) \Lambda_{\langle i-\ell\rangle} e^{-\omega(N-1)m} \end{bmatrix} \quad (88)$$

and

$$\mathbf{F}\boldsymbol{\Psi}(\ell) = \kappa^2 \begin{bmatrix} \sum_{m,i=0}^{N-1} w_i(m) \bar{\Lambda}_{\langle i-\ell\rangle} \\ \sum_{m,i=0}^{N-1} w_i(m) \bar{\Lambda}_{\langle i-\ell\rangle} e^{-\omega m} \\ \vdots \\ \sum_{m,i=0}^{N-1} w_i(m) \bar{\Lambda}_{\langle i-\ell\rangle} e^{-\omega(N-1)m} \end{bmatrix} . \quad (89)$$

Therefore, the FFT kth pin output is given by

$$r_k(\ell) = \kappa^2 \sum_{m=0}^{N-1} \sum_{i=0}^{N-1} x_m(i) \Lambda_{\langle i-\ell\rangle} e^{-\omega k m} + \kappa^2 \sum_{m=0}^{N-1} \sum_{i=0}^{N-1} w_i(m) \bar{\Lambda}_{\langle i-\ell\rangle} e^{-\omega k m}$$

$$= \kappa \sum_{i=0}^{N-1} \Lambda_{\langle i-\ell\rangle} d_k(i) + \kappa^2 \sum_{i=0}^{N-1} \sum_{m=0}^{N-1} \bar{\Lambda}_{\langle i-\ell\rangle} w_i(m) e^{-\omega k m}. \quad (90)$$

REFERENCES

[1] M. Ahmed, S. Boussakta, B. Sharif, and C. Tsimenidis, "OFDM based on low complexity transform to increase multipath resilience and reduce PAPR," *IEEE Trans. Signal Process.*, vol. 59, pp. 5994–6007, Dec. 2011.

[2] Radio roadcasting systems; digital audio broadcasting (DAB) to mobile, portable and fixed receivers, ETS Standard 300 401, 1995.

[3] Digital video broadcasting (DVB); framing structure, channel coding and modulation for digital terrestrial television, ETSI Standard EN 300 744 v1.6.1, 2008.

[4] IEEE Standard for Local and metropolitan area networks Part 16: Air Interface for Broadband Wireless Access Systems Amendment 3: Advanced Air Interface, IEEE Standard 802.16m, 2011.

[5] LTE; Evolved Universal Terrestrial Radio Access (E-UTRA) and Evolved Universal Terrestrial Radio Access Network (E-UTRAN); Overall description, 3GPP Standard TS 36.300, 2011.

[6] Digital video broadcasting (DVB); frame structure channel coding and modulation for a second generation digital transmission system for cable systems (DVB-C2), ETSI Standard EN 302 769, 2010.

[7] Asymmetric digital subscriber line transceivers 2 (ADSL2) – extended bandwidth (ADSL2plus), ITU-T standard G.992.5, 2009.

[8] IEEE Standard for Broadband over Power Line Networks: Medium Access Control and Physical Layer Specifications, IEEE Standard 1901, 2010.

[9] S. Wang, S. Zhu, and G. Zhang, "A Walsh-Hadamard coded spectral efficient full frequency diversity OFDM system," *IEEE Trans. Commun.*, vol. 58, pp. 28–34, Jan. 2010.

[10] R. Schober and L. Lampe, "Differential modulation diversity," *IEEE Trans. Veh. Technol*., vol. 51, no. 6, pp. 1431–1444, Nov. 2002.

[11] L. Lampe and R. Schober, "Differential modulation diversity for OFDM," in *Proc. 2001 Int. OFDM-Workshop*, pp. 1–5.

[12] A. Hazmi, J. Rinne,and M. Renfors, "An enhanced impulse burst cancellation method using pilots and soft bits in OFDM based systems," in *Proc. 2004 IEEE Workshop on Signal Processing Advances in Wireless Communications*, pp. 373–376.

[13] A. Hazmi, J. Rinne, and M. Renfors, "Performance evaluation of symbol synchronization in OFDM systems over impulsive noisy channels," in *Proc. 2004 IEEE Vehicular Technology Conf.*, pp. 1782–1786.

[14] A. Hazmi, J. Rinne, M. Renfors, J. Vesma, T. Auranen, P. Talmola, and J. Henriksson, "Mitigation techniques for high power and long duration interference in DVB-T/H systems," in *Proc. 2007 IEEE Int. Symp. Personal, Indoor and Mobile Radio Communications*, pp. 1–5.

[15] S. Zhidkov, "Analysis and comparison of several simple impulsive noise mitigation schemes for OFDM receivers," *IEEE Trans. Commun*., vol. 56, pp. 5–9, Jan. 2008.

[16] I. Mann, S. McLaughlin, W. Henkel, R. Kirkby, and T. Kessler, "Impulse generation with appropriate amplitude, length, inter-arrival, and spectral characteristics," *IEEE J. Sel. Areas Commun.*, vol. 20, pp. 901–912, Jun. 2002.

[17] S. Zhidkov, "Impulsive noise suppression in OFDM based communication systems," *IEEE Trans. Consum. Electron*., vol. 49, pp. 944–948, Nov. 2003.

[18] R. Pighi, M. Franceschini, G. Ferrari, and R. Raheli, "Fundamental performance limits of communications systems impaired by impulse noise," *IEEE Trans. Commun*., vol. 57, pp. 171–182, Jan. 2009.

[19] F. Abdelkefi, A. Gabay, and P. Duhamel, "Impulse noise cancellation in multicarrier transmission," *IEEE Trans. Commun*. vol. 53, pp. 94–106, Jan. 2005.

[20] S. V. Zhidkov, "Performance analysis and optimization of OFDM receiver with blanking nonlinearity in impulsive noise environment," *IEEE Trans. Veh. Technol*., vol. 55, pp. 234–242, Jan. 2006.

[21] M. Zimmermann and K. Dostert, "Analysis and modeling of impulsive noise in broad-band powerline communications," *IEEE Trans. Electromagn. Compat*., vol. 44, pp. 250–258, Feb. 2002.

[22] Y. Ma, P. So, and E. Gunawan, "Performance analysis of OFDM systems for broadband power line communications under impulsive noise and multipath effects," *IEEE Trans. Power Del.,* vol. 20, pp. 674–682, Apr. 2005.

[23] A. Al-Dweik, A. Hazmi, B. Sharif, and C. Tsimenidis, "Efficient interleaving technique for OFDM system over impulsive noise channels," in *Proc. 2010 IEEE PIMRC*, pp. 167–171.

[24] S. Nayyef, A. Al-Dweik, A. Hazmi, B. Sharif, and C. Tsimenidis, "An efficient technique for OFDM systems over fading channels impaired by impulsive noise," in *Proc. 2012 IEEE VTC*.

[25] A. D. S. Jayalath and C. Tellambura, "Use of data permutation to reduce the peak-to-average power ratio of an OFDM signal," *Wirel. Commun. Mob. Comput.*, vol. 2, pp. 187–203, 2002.

[26] A. Al-Dweik, A. Hazmi, Y. Sedki, B. Sharif, and C. Tsimenidis, "Blind iterative frequency offset estimator for OFDM systems," *IET Commun.*, vol. 4, no. 16, pp. 2008–2019, Nov. 2010.

[27] Y. Li and G. Stuber, *Orthogonal Frequency Division Multiplexing for Wireless Communications*. Springer, 2006.

[28] A. Al-Dweik, S. Younis, A. Hazmi, B. Sharif, and C. Tisimendis, "An efficient OFDM symbol timing estimator using power difference measurements," *IEEE Trans. Veh. Technol.*, vol. 61, pp. 509–520, Feb. 2012.

[29] D. Middleton, "Canonical and quasi-canonical probability models of class A interference," *IEEE Trans. Electormagn. Compat*., vol. EMC-25, no. 2, pp. 76–106, May 1983.

[30] M. Ghosh, "Analysis of the effect of impulse noise on multicarrier and single carrier QAM systems," *IEEE Trans. Communn.*, vol. 44, pp. 145–147, Feb. 1996.

[31] E. Al-Dalakta, A. Al-Dweik, A. Hazmi, C. Tsimenidis, and B. Sharif, "PAPR reduction usingmMaximum cross correlation," *IEEE Commun. Lett.*, vol. 16, pp. 2032–2035, Dec. 2012.

[32] B. Sklar, *Digital Communications: Fundamentals and Applications*. Prentice-Hall PTR, 2001

[33] V. Witkovsky, "Computing the distribution of a linear combination of inverted Gamma variables," *Kubernetika*, vol. 37, pp. 70–90, 2001.

[34] M. McCloud, "Analysis and design of short block OFDM spreading matrices for use on multipath fading channels," *IEEE Trans. Commun.,* vol. 53, pp. 656–665, Apr. 2005.

[35] Z. Wang and G. Giannakis, "A simple and general parameterization quantifying performance in fading channels," *IEEE Trans. Commun.,* vol. 51, pp. 1389–1398, Aug. 2003.

[36] Y. Jiang, M. Varanasi, and J. Li, "Performance analysis of ZF and MMSE equalizers for MIMO systems: an in-depth study of the high SNR regime," *IEEE Trans. Inf. Theory,* vol. 57, pp. 2008–202, Apr. 2011.

[37] X. Huang, "Multipath diversity of precoded OFDM with linear equalization, in *Proc. IEEE Int. Conf. Commun.,* pp. 1307–1311, May 2008.

[38] A. Mengi and A. Vinck, Successive impulsive noise suppression in OFDM," in *Proc. 2010 IEEE Int. Symp. Power Line Communications and Its Applications*, pp. 33–37, Mar. 2010.

[39] C. H. Yih, "Iterative interference cancellation for OFDM signals with blanking nonlinearity in impulsive noise channels," *IEEE Signal Process. Lett*., vol. 19, pp. 147–150, Mar. 2012.

[40] H. Eghbali, S. Muhaidat, and N. Al-Dhahir, "A novel receiver design for single-carrier frequency domain equalization in broadband wireless networks with amplify-and-forward relaying," *IEEE Trans. Wireless Commun.*, vol. 10, pp. 721–727, Mar. 2011.

[41] A. Al-Dweik, "A non data aided symbol timing recovery technique for OFDM systems," *IEEE Trans. Commun.,* vol. 1, pp. 3740, Jan. 2006.

[42] Y. P. Lin and S. M. Phoong, "BER minimized OFDM systems with channel independent precoders," *IEEE Trans. Signal Process.,* vol. 51, no. 9, pp. 2369–2380, Sep. 2003.

[43] T. Zheng, M. Raugi, and M. Tucci, "Time-invariant characteristics of naval power-line channels," *IEEE Trans. Power Del*., vol. 27, no. 2, pp. 858–865, Apr. 2012.

[44] A. Tomasoni, D. Gatti, S. Bellini, M. Ferrari, and M. Siti, "Efficient OFDM channel estimation via an information criterion," *IEEE Trans. Wireless Commun.*, vol. 12, no. 3, pp. 1352–1362, Mar. 2013.

[45] X. Doukopoulos and G. Moustakides, "Blind adaptive channel estimation in OFDM systems," *IEEE Trans. Wireless Commun.*, vol. 5, no. 7, pp. 1716–1725, July 2006.

Maysam Mirahmadi (M'09) received the B.Sc. and M.Sc. degrees in Electrical Engineering from Amirkabir University of Technology (Tehran Polytechnic), Tehran, Iran, in 2004 and 2007, respectively. From 2007 to 2009, he was a Senior Designer at Kavoshkam R&D Group, Tehran, Iran. In 2013, he received the Ph.D. degree from the University of Western Ontario. Currently he is working as a research scientist at Canada Research and Development Center (CRDC), IBM Canada Ltd. His current research interests include wireless communications, optimized computations and high performance computing.

Arafat Al-Dweik (S'9–M'01–SM'04) received the M.S. and Ph.D. degrees in electrical engineering from Cleveland State University, Cleveland, OH, USA in 1998 and 2001, respectively. From 2003 to 2013 he was an Assistant and then Associate Professor at the Department of Electrical and Computer Engineering at Khalifa University, UAE, and he recently joined the School of Engineering at University of Guelph, Guelph, ON, Canada, and he holds an Adjunct Research Professor position at Western University, London, ON, Canada. Dr. Al-Dweik has several years of industrial experience in the USA, recipient of the Fulbright Scholarship, and has been awarded several awards and research grants. He is also a Senior Member of the IEEE and Associate Editor of the IEEE TRANSACTIONS ON VEHICULAR TECHNOLOGY. The main research interests of Dr. Al-Dweik include Wireless Communications, synchronization techniques, OFDM technology, modeling and simulation of communication systems, error control coding, and spread spectrum systems.

Abdallah Shami (M'03–SM'09) received the B.E. degree in Electrical and Computer Engineering from the Lebanese University, Beirut, Lebanon in 1997, and the Ph.D. Degree in Electrical Engineering from the Graduate School and University Center, City University of New York, New York, NY in September 2002. In September 2002, he joined the Department of Electrical Engineering at Lakehead University, Thunder Bay, ON, Canada as an Assistant Professor. Since July 2004, he has been with Western University, Canada where he is currently an Associate Professor in the Department of Electrical and Computer Engineering. His current research interests are in the area of network optimization, cloud computing, and wireless networks. Dr. Shami is an Editor for IEEE COMMUNICATIONS SURVEYS AND TUTORIALS and has served on the editorial board of IEEE COMMUNICATIONS LETTERS (2008-2013). Dr. Shami has chaired key symposia for IEEE GLOBECOM, IEEE ICC, IEEE ICNC, and ICCIT. Dr. Shami is a Senior Member of IEEE.